Oceanic Data Analysis Using a General Circulation Model. Part I: Simulations*

ELI TZIPERMAN

Department of Environmental Sciences and Energy Research, The Weizmann Institute of Science, Rehovot, Israel

WILLIAM CARLISLE THACKER AND ROBERT BRYAN LONG

Atlantic Oceanographic and Meteorological Laboratory, Miami, Florida

SHOW-MING HWANG

Cooperative Institute for Marine and Atmospheric Sciences, Miami, Florida

(Manuscript received 5 December 1990, in final form 29 January 1992)

ABSTRACT

This paper deals with the solution of inverse problems involving complex numerical models of the oceanic general circulation and large datasets. The goal of these inverse problems is to find values for model inputs consistent with a steady circulation and, at the same time, consistent with the available data. They are formulated as optimization problems, seeking values for the model's inputs that minimize a cost function measuring departures from steady state and from data. The two main objectives of this work are 1) to examine the feasibility of solving inverse problems involving a realistic numerical model of the oceanic general circulation and 2) to understand how the optimization uses various data to calculate the desired model parameters.

The model considered here is similar to the primitive equation model of Bryan and of Cox, the principal difference being that here the horizontal momentum balance is essentially geostrophic. The model's inputs calculated by the optimization consist of surface fluxes of heat, water, and momentum, as well as the eddy-mixing parameters. In addition, optimal estimates for the hydrography are obtained by requiring the hydrography to be consistent with both other types of data and the model's dynamics.

In the examples presented here, the data have been generated by the model from known inputs; in some cases, simulated noise has been added. The cost function is a sum of terms quadratic in the differences between the data and their model counterparts and terms quadratic in the temperature and salinity time rate of change as evaluated using the model equations. The different inverse problems considered differ in the choice of the model inputs calculated by the optimization and in the data used in the cost function. Optimal values of the model's inputs are computed using a conjugate-gradient minimization algorithm, with the gradient computed using the so-called adjoint method.

In examples without added noise, solutions for the model inputs were found efficiently and accurately. This was not the case when simulated data with randomly generated noise were used. Amplification of noise was especially felt in regions of deep-water formation due to the strong vertical mixing in these regions. Away from deep-water formation regions, the performance of the optimization with noisy data was still not satisfactory, possibly due to bad conditioning of the problem. The conditioning of the optimization and the difficulties due to the noise amplification are further discussed in Part II of this work using real oceanographic data for the North Atlantic Ocean.

1. Introduction

The recent years have witnessed rapid progress in methods of making oceanographic observations, as well as in numerical general circulation models (GCMs). Yet, there is still a gap between the models used for simulations and the models used to analyze the existing observations. Today's GCMs are run with high, eddy-resolving resolution, realistic geometry, and complex dynamics (Semtner and Chevrin 1988). They require, however, as inputs the surface forcing by the wind stress and by air–sea fluxes of heat and fresh water, as well as other model parameters, such as eddy-mixing coefficients. Unfortunately, these inputs are among the least well-known aspects of the oceanic circulation. The vast body of hydrographic (temperature and salinity) and other oceanographic data available from years of measurements can only be used by the numerical models for model validation, mostly through a qualitative comparison between model results and data.

* Contribution No. 29, Department of Environmental Sciences and Energy Research, The Weizmann Institute of Science.

Corresponding author address: Dr. Eli Tziperman, The Weizmann Institute of Science, Department of Environmental Sciences, 76100 Rehovot, Israel.

Studies using inverse methods (Stommel and Schott 1977; Wunsch 1978; Olbers et al. 1985; Mercier 1989; Provost and Salmon 1986) have attempted to circumvent the need to specify poorly known model inputs by using our knowledge of oceanic dynamics, mass, and in particular, tracer conservation. In these studies, relatively simple models have been used in analyzing the data, often focusing attention on the calculation of the circulation, though this is only one part of a larger problem. Surface fluxes of heat, water, and momentum are also of interest, while information about them is mostly unreliable. We would like to improve the estimates of surface fluxes by using information contained in the hydrographic data. We would also like to extract information about mixing processes that are important for the general circulation. And as the hydrographic data are often noisy, aliased, and incomplete, another goal is to obtain better estimates for the temperature and salinity fields. The larger problem, then, is to estimate flow fields, hydrography, surface forcing fields, and mixing parameters in a manner consistent with all available data and with the full dynamics of a GCM.

Computational limitations have restricted the models used in inverse problems to relatively coarse resolution and/or to local, non–mass-conserving dynamics and have prevented consideration of all aspects of this larger problem. The purpose of this paper is to examine the opportunities for relaxing these restrictions offered by more efficient mathematical methods. In particular, when inverse problems are formulated as optimization problems requiring the minimization of a cost function, conjugate-gradient minimization algorithms, together with the adjoint method for computing the gradient of the cost function with respect to the unknowns (Le Dimet and Talagrand 1986; Thacker and Long 1988; Tziperman and Thacker 1989), make feasible, at least in principle, the solution of inverse problems based on GCMs. Using this methodology, we wish to explore in this work the possibility of posing meaningful and solvable inverse problems using sophisticated general circulation models of the oceanic circulation.

The present work deals with problems related to the application of the adjoint method to the study of the steady-state oceanic general circulation using a realistic numerical oceanic general circulation model (OGCM) and hydrographic data. In this paper, we deal with inverse problems posed using simulated data with and without added noise, while in Tziperman et al. (1992, Part II hereafter), we use North Atlantic data and model to examine the challenges posed by real oceanographic data that may be both noisy and inconsistent with the model used to analyze it. The preset paper, dealing with simulated data, has three specific objectives.

Our first objective, somewhat technical yet far from trivial, is to demonstrate the feasibility of using the adjoint method for calculating the gradient of the cost function with a complex OGCM. A crucial component of the method for solving inverse problems based on complex numerical models is the adjoint model, which is used to efficiently and accurately compute the gradient of the cost function with respect to all model inputs. So far, uses of the adjoint method in physical oceanography have been limited to relatively simple models, certainly far simpler than a full GCM. Tziperman and Thacker (1989) have used it with a barotropic vorticity-equation model; Thacker and Long (1988) with a simple equatorial-wave model; Sheinbaum and Anderson (1990) with a one-layer, linear, reduced-gravity model; Wunsch (1988) with a simple box model; and Schröter (1989) with a one-dimensional, time-dependent model. Until now, however, the construction and use of an adjoint for a sophisticated GCM have not been shown to be feasible. An adjoint for the Bryan (1969) and Cox (1984) primitive equation model has been constructed at the Atlantic Oceanographic and Meteorological Laboratory (Long et al. 1989). The development of this adjoint code posed a rather challenging technical problem, and although this is not the focus of the work presented here, we wish to emphasize that all specific experiments carried out here serve to demonstrate that the construction of an adjoint for a complex OGCM is feasible. The model used for the present study is a modified version of the Bryan–Cox model, and its adjoint is a modification of that adjoint. Once the gradient of the cost function can be calculated efficiently, it still remains to be decided how this tool is to be used to formulate and solve specific inverse problems. That issue is our main focus and forms the essence of our two remaining main objectives.

Our second objective is to gain some understanding of the way the optimization uses various types of data in order to infer unknown model parameters. This is done by considering a series of inverse problems, from very simple to more complex ones, and carefully examining the results of each experiment. When difficulties are encountered, the knowledge of the "true" solution (i.e., the model-generated simulated data) is a major advantage in trying to understand the source of these difficulties.

Finally, by understanding how the different data are used to calculate model parameters, we try to find out what model parameters may be determined using hydrographic data and a GCM. The answer to this question may, of course, depend on the specific form of the inverse problem (i.e., the form of the cost function being minimized). But although our experiments are not exhaustive in that sense, they still give some insight into the problem. Previous work (Tziperman and Thacker 1989) has shown that care must be taken when calculating model parameters from data. The successful calculation of model parameters critically depends on the type of data available. Trying to calculate parameters using insufficient or inadequate data may result

in the wrong solution for the desired parameters. Tziperman and Thacker found, for example, using a simple barotropic quasigeostrophic (QG) model, that calculating both wind forcing and mixing coefficients from vorticity observations results in a nonunique solution for these parameters, indicating that vorticity data are not sufficient for resolving both wind and mixing coefficients.

The methodology used here was previously presented by Tziperman and Thacker (1989), using a simple barotropic QG model and simulated observations. It is, therefore, useful to explain why another study using simulated observations is needed (beyond, of course, the need to demonstrate the technical possibility of constructing an adjoint for a complex GCM). The novelty of this work is not in the number of unknowns calculated (roughly the same here and in Tziperman and Thacker), but in the complexity of the model used. The present model, being a full GCM, is a 3D model with equations for the velocity, temperature, and salinity fields as opposed to the simple 2D vorticity equation of the initial study. The present model is forced at the surface by wind stress and by heat and freshwater fluxes as opposed to wind curl only in the QG model. There are, therefore, many more different types of model inputs to be calculated within an inverse study using this model (temperature, salinity, heat fluxes, evaporation minus precipitation, and wind-stress components) than exist in a simple QG model (vorticity and wind curl only). As a result of the model complexity and more varied unknowns, the optimization (inverse) problem is also more challenging. For example, given that the number of unknowns is the same for the QG model and the present GCM, the problem of calculating these unknowns may be expected to be significantly more difficult for two reasons. The first is the far more complex nonlinearity of the model equations. In the QG model nonlinearity was simply due to vorticity advection, while here the nonlinear advection terms in the temperature equation are supplemented with the nonlinear coupling of the temperature and salinity fields to the density field and, in turn, the effects of the density field on the pressure terms in the momentum equations. In addition to the nonlinearity, the existence of many types of unknowns results in a more difficult optimization problem due to the problem of preconditioning, discussed in detail by Tziperman et al. (1992).

The far more sophisticated dynamics used here, therefore, raise many new questions and expected difficulties that need to be discussed within the framework of a controlled experiment before applying the model and method to real North Atlantic data as we do in Part II. The experience and understanding gained in these controlled experiments should help in critically evaluating the results of the North Atlantic study using the same methodology and model. Only through this interaction between simulations and inversions of real oceanographic data can one learn the possibilities and difficulties of a new methodology. The comparison of simulations and real data analysis will be reiterated several times below and while describing the North Atlantic model.

The present model, like most previous inverse models of the oceanic general circulation, is based on steady dynamics. Yet, it is far from obvious that even the time-averaged circulation can be described by a steady model. The "ultimate" inverse model should certainly be based on eddy-resolving time-dependent dynamics, with the average of the model fields somehow fitted to the averaged data. Such an inverse calculation, however, is not feasible with today's computers, which can hardly deal with direct simulations of the ocean using eddy-resolving models. The use of steady models for inverse studies at this stage has, therefore, two practical justifications. First, it makes sense to advance toward a time-dependent inverse model in stages by developing and learning the needed methodologies and possible difficulties before approaching the full problem. In addition, a general rule for any work trying to explain observations is to first try to explain the data using the simplest model possible; only if inconsistencies between model and data are found, is one justified in further complicating the model (in the oceanographic case, by making the model, for example, time dependent). This work may be viewed as an effort to carry the steady assumption to its limit by developing a methodology that enables use of the most sophisticated steady model within an inverse calculation, a target not possible using previous methodologies. The steady-state assumption is further discussed when the model and method presented here are applied to real North Atlantic data in Part II.

In the following sections, the GCM used for this study is presented (section 2); then some of the details of the adjoint method as applied to the present model are described (section 3). The numerical examples using the model and the adjoint method are described in section 4, and concluding remarks are made in section 5.

2. The model

a. Model equations

The GCM used in this study is based on the well-known primitive equation (PE) model of Bryan (1969) and Cox (1984) and shares many of its features. The principal difference between the models is in the momentum equations, for in our model, time-derivative terms and advection of momentum have been neglected and dissipation is approximated by Rayleigh friction. This approximation has been termed the "planetary geostrophic" approximation and is appropriate for modeling the large-scale circulation (Salmon 1986; Colin de Verdiere 1988). There are several advantages in using the simplified model rather than the

full PE model for inverting hydrographic data, and these will be discussed in section 3.

As the original model is well documented (Bryan 1969; Cox 1984), attention here will focus on the modifications. Spherical coordinates are used, with a the radius of the earth, ϕ latitude, λ longitude, and z the local vertical coordinate. The rotation rate of the earth is denoted by Ω, and the Coriolis parameter is $f = 2\Omega \sin\phi$; T, S, and P denote the temperature, salinity, and pressure; ρ, ρ_0 denote the density and a constant reference density. Following Bryan's (1969) notations, we also let

$$m = \sec\phi; \quad u = (a/m)d\lambda/dt; \quad v = ad\phi/dt; \quad w = dz/dt. \quad (1)$$

The model equations are then as follows. An advection diffusion equation is used for the temperature:

$$T_t + \frac{m}{a}[(uT)_\lambda + (vT/m)_\phi] + (wT)_z, = K_h\nabla_H^2 T + K_v T_{zz}, \quad (2)$$

and a similar equation is used for the salinity. The model is hydrostatic and mass conserving:

$$P_z = -g\rho; \quad a^{-1}[u_\lambda + (v/m)_\phi] + w_z = 0, \quad (3)$$

and a polynomial approximation to the equation of state is used to relate temperature, salinity, pressure, and density (Bryan and Cox 1972),

$$\rho = \rho(T, S, P). \quad (4)$$

The simplified momentum equations used are

$$-fv = -ma^{-1}(P/\rho_0)_\lambda - ru + \tau^x/D_e, \quad (5a)$$

$$fu = -a^{-1}(P/\rho_0)_\phi - rv + \tau^y/D_e, \quad (5b)$$

where r is a small Rayleigh friction coefficient, included in order to allow satisfying the no-normal flow boundary conditions at horizontal boundaries (landmasses). Because there is no vertical diffusion of momentum in the model's physics, the wind (τ^x, τ^y) is taken as a body force that is different from zero only within the Ekman layer, rather than using it as an upper boundary condition for the momentum equations. The Ekman layer is assumed to have a constant depth D_e throughout the domain and is taken to be the uppermost level of the model, so that its thickness is $D_e = dz_1$. A no-slip boundary condition is used for the velocity field at the boundaries. Such a condition is, in fact, not supported by the Rayleigh friction used in the momentum equations but may be regarded as a subgrid parameterization of mixing processes near the boundaries that are not explicitly modeled. Note that for the momentum equations to be nearly geostrophic, as desired, the friction coefficient must be much smaller than the Coriolis parameter: $r \ll f$.

The absence of the inertial terms in the momentum equations can be justified for most regions of the World Ocean, except perhaps in western boundary current regions, where the nonlinear terms in the momentum equations may be important. (Although even in these regions, the simplified equations may hold for the yearly averaged, rather than instantaneous, circulation.)

Surface fluxes of heat and fresh water (the latter in the form of an equivalent salt flux) are specified at the surface as boundary conditions for the temperature and salinity,

$$K_v T_z = \mathscr{H}; \quad K_v S_z = S_0(E - P), \quad \text{at} \quad z = 0. \quad (6)$$

A Richardson number parameterization is used for the vertical-mixing coefficient (Pacanowski and Philander 1981):

$$K_v = \begin{cases} K_{\max}/(1 + 5\ \mathrm{Ri})^3 + K_{v0} & \text{if,} \quad \mathrm{Ri} > 0 \\ K_{\max} + K_{v0}, & \text{otherwise,} \end{cases} \quad (7)$$

where $\mathrm{Ri} = (g\rho_z/\rho_0)/(u_z^2 + v_z^2)$ is the Richardson number, the background diffusivity is given by K_{v0}, and the strength of the vertical mixing in regions where shear instability or unstable vertical density profiles are expected is governed by the parameter $K_{\max} = 50$ cm^2 s^{-1}. The background diffusivity K_{v0} is set to 1 cm^2 s^{-1} in order to obtain the simulated observations and is treated as an unknown in the optimizations presented below, while $K_{\max}$ is chosen to remain fixed at the value specified above. When running the model to steady state in a closed basin, the vertical diffusivity was found to be equal to the background diffusivity K_{v0} in most locations, except for regions of water-mass formation that were often slightly statically unstable, so that $\mathrm{Ri} < 0$, and the diffusivity was found to be equal to its maximum value. The large maximal vertical mixing coefficient, $K_{\max}$, was found to be sufficient for preventing grossly unstable profiles from forming. Note that this large coefficient is used only in regions of unstable or nearly unstable density profile and does not affect the temperature equation elsewhere. No convective adjustment is included in the model in order to mix statically unstable regions (such regions are vertically mixed in the original model at every time step). Clearly, our vertical convection parameterization is far from ideal, allowing in principle the existence of (slightly) unstable regions. We are forced to use it, however, as the original parameterization seems to cause serious difficulties in the optimization process, as we shall see in section 2b. The inability of the optimization to deal with the convective overturning process is one of our important conclusions, and better solutions to this problem may have to be developed in later studies. The aforementioned parameterization of vertical mixing was chosen because it is smooth and differentiable with respect to the initial conditions for temperature and salinity, and we shall return to this

point later when describing the numerical examples in section 4.

b. Time stepping

In order to advance the model in time, we need to eliminate the unknown surface pressure terms in the momentum equations. This is done using a procedure similar to that used in the original PE model. First, separate all quantities into baroclinic and barotropic parts, for example,

$$u = \bar{u} + u'; \quad \bar{u} \equiv \frac{1}{H}\int_{z=-H}^{0} u dz; \quad \overline{u'} = 0. \quad (8)$$

The pressure can be calculated from the hydrostatic equation (3) in terms of the interior density field and the unknown pressure at the surface $P_s(x, y)$

$$P(x, y, z) = P_s(x, y) + \frac{-g}{\rho_0}\int_{z}^{0} dz'\rho(x, y, z'). \quad (9)$$

Next, subtract the vertically averaged (barotropic) components of all terms in the momentum equations (5a,b). Because these equations are linear, the resulting equations for the baroclinic components are exactly equivalent to (5a,b), except that primes are added to all quantities in these equations. The baroclinic velocities can now be solved for directly in terms of the known wind forcing and baroclinic pressure gradients that do not include the contribution from the unknown surface pressure,

$$u' = \frac{1}{f^2 + r^2}[f[-a^{-1}(P'/\rho_0)_\phi + \tau'^y/D_e] + r[-ma^{-1}(P'/\rho_0)_\lambda + \tau'^x/D_e]] \quad (10a)$$

$$v' = \frac{1}{f^2 + r^2}[r[-a^{-1}(P'/\rho_0)_\phi + \tau'^y/D_e] - f[-ma^{-1}(P'/\rho_0)_\lambda + \tau'^x/D_e]]. \quad (10b)$$

To solve for the barotropic velocities, define a barotropic streamfunction,

$$\psi_x = \int_{z=-H}^{0} v dz; \quad -\psi_y = \int_{z=-H}^{0} u dz, \quad (11)$$

and derive an equation for it as follows. First, take the curl of the momentum equations: curl(5a, 5b) = $[5b]_\lambda - ([5a]/m)_\phi$. Next, separate the velocities appearing in the resulting equation into the barotropic parts written in terms of ψ and the baroclinic part that is known from (10a,b); move all wind terms and baroclinic terms to the rhs to find the desired equation for the streamfunction,

$$r\left[\left(\frac{m}{aH}\psi_\lambda\right)_\lambda + \left(\frac{1}{aHm}\psi_\phi\right)_\phi\right] - \left(\frac{f}{aH}\psi_\lambda\right)_\phi + \left(\frac{f}{aH}\psi_\phi\right)_\lambda = Z(\lambda, \phi), \quad (12a)$$

where

$$Z(\lambda, \phi) = [\tau^x/D_e m + fv'/m - ru'/m]_\phi - [\tau^y/D_e - fu' - rv']_\lambda. \quad (12b)$$

In the finite-difference formulation of the model, the vorticity forcing function $Z(\lambda, \phi)$ (12b) is evaluated at the uppermost grid point where all primed quantities are defined (the vorticity driving function, Z, can be shown to be independent of depth throughout the water column, but it may not be defined at some horizontal locations below the depth of the topography).

The model is advanced in time as follows. Given the temperature and salinity fields at a given time, the density field is calculated using the equation of state. Then, the baroclinic pressure field is found from the density using the hydrostatic relation. Next, the baroclinic velocities at the present time are evaluated using (10a,b), and the barotropic component of the velocities is evaluated by solving the equation for the streamfunction (see Appendix). Finally, the full velocity field is formed by combining the baroclinic and barotropic velocities and is used to advance the temperature and salinity equations (2) in time.

3. Cost function, adjoint model, and optimization algorithm

A variety of inverse problems may be formulated using a GCM. In every case, these problems require adjusting some of the model's inputs to bring the model's solution into agreement with observations and with our prejudice of what the ocean physics should be. The problem is posed such that, when the optimal model inputs are found, a cost function, measuring the agreement of the model solution with the observations and with the dynamic assumptions made, is at its minimum. The particular data being studied, together with the dynamics assumed to hold, should dictate the precise statement of the inverse problem and, consequently, the definition of the cost function to be minimized.

For the problem in which we are interested, the analysis of the oceanic general circulation, the data may include various types. There is, of course, the hydrographic data (temperature and salinity), possibly some direct velocity measurements, air–sea fluxes, wind data, etc. The hydrographic (and other) data are meant to represent a many-year average of the observed fields, and we assume that the ocean as represented by these data is in a steady state. The cost function is therefore defined as the sum of two terms, the first representing model–data differences and the second measuring the distance of the model equations from a steady state. Our purpose is then to find the temperature, salinity, wind forcing, and surface fluxes of heat and fresh water that best fit the available hydrographic data and that are also as close as possible to a steady-state solution of the GCM. The cost function is minimized subject

to the constraints posed by all nonprognostic model equations and boundary conditions. That is, the steady-state and data constraints are handled as soft constraints, and all other model equations and boundary conditions are used as hard constraints.

The cost function, together with the model equations described in section 2, are used to form a Lagrange function from which the adjoint model equations are derived. The gradient of the cost function with respect to the different model inputs can then be efficiently calculated using the adjoint model. The optimization procedure used to minimize the cost function proceeds as follows. The GCM is run, and the cost function is calculated; then the adjoint model is run, and the gradient is calculated; this gradient is then used within a conjugate-gradient algorithm to find a new guess for the model parameters that reduces the value of the cost function. This process is repeated until the cost function is minimized, and the optimal values of all model inputs are calculated. Each of these stages will now be discussed briefly, refraining from details that can be found elsewhere (Tziperman and Thacker 1989).

a. The cost function

The terms in the cost function measuring the deviation of the model inputs from the observations are taken to be the sum of squares of the differences between model inputs and the observations available for these inputs, weighted according to the estimated error in the observations. The deviation of the model solution from steady state is measured by the sum of squares of the temporal derivative terms in the model equations for the temperature and salinity. The data misfit term at a grid location (ijk), for the temperature, for example, is proportional to $(\hat{T}_{ijk} - T_{ijk}^{n=0})^2$, where $\hat{T}_{ijk}$ is the data value and $T_{ijk}^{n=0}$ is the temperature calculated by the optimization and used as initial condition for the model run. The temporal derivatives appearing in the cost function are evaluated by stepping the model a single time step, from the initial conditions $T_{ijk}^{n=0}$ calculated by the optimization procedure at any given iteration: $T_{t,ijk} = (T_{ijk}^{n=1} - T_{ijk}^{n=0})/\Delta t$. Denoting with a caret ($\hat{}$) the observations for the various fields, the cost function can be written as

$$
\begin{aligned}
J = & \sum_{i,j,k} [\bar{W}_{ijk}^{T}(T_{t,ijk})^2 + \bar{W}_{ijk}^{S}(S_{t,ijk})^2] \\
& + \sum_{i,j,k} [W_{ijk}^{T}(\hat{T}_{ijk} - T_{ijk}^{n=0})^2 + W_{ijk}^{S}(\hat{S}_{ijk} - S_{ijk}^{n=0})^2] \\
& + \sum_{i,j,k} [W_{ijk}^{U}(\hat{u}_{ijk} - u_{ijk})^2 + W_{ijk}^{V}(\hat{v}_{ijk} - v_{ijk})^2] \\
& + \sum_{i,j} \{W_{i,j}^{\tau}[(\hat{\tau}_{ij}^{x} - \tau_{ij}^{x})^2 + (\hat{\tau}_{ij}^{y} - \tau_{ij}^{y})^2]\} \\
& + \sum_{i,j} [W_{i,j}^{\mathscr{H}}(\hat{\mathscr{H}}_{ij} - \mathscr{H}_{ij})^2\} \\
& + W_{i,j}^{E-P}\{[(\hat{E} - \hat{P}_{ij}) - (E - P_{ij})]^2\}. \qquad (13)
\end{aligned}
$$

The weights W_{ijk}^{T}, etc., determine the relative importance of the different terms of the cost function (note that the important factor is the relative magnitudes of the different weights, and not the absolute value of a given weight). A complete statement of the cost function should involve weighting by the inverse error covariance matrix for the data used in the cost function. Such a matrix, however, is quite large and difficult to use for a large-scale optimization involving an OGCM; therefore, we resort to the commonly used diagonal weighting by the weights appearing in (13). Each temperature or salinity data term in the cost function is weighted by the inverse of squared error for that data point, as well as by the volume of the grid box represented by the particular data point divided by the volume of the ocean. The error in the hydrographic data was specified as a function of depth only, based on the rms amplitude of the simulated noise added to the simulated data. The weights can therefore be written as

$$
W_{ijk}^{T} = \frac{1}{[\epsilon_k(T)]^2} \frac{dx_i\, dy_j dz_k}{\text{volume}}, \qquad (14)
$$

where $\epsilon_k(T)$ is the specified amplitude of the randomly generated temperature noise at level k (see section 4). Similarly, the terms in the cost function involving data for the surface forcing fields are weighted by the inverse mean-squared error times the volume of the uppermost grid box directly affected by these fluxes, $W_{ij}^{\mathscr{H}} = (1/\epsilon(\mathscr{H})^2) \times (dx_i\, dy_j dz_1/\text{volume})$.

A more difficult problem is posed by the weighting of the steady penalty terms in the cost function, specified by $\bar{W}_{ijk}^{T}$ and $\bar{W}_{ijk}^{S}$. It is not obvious how these weights should be set a priori, as we do not know what the expected error in these terms is. We have adopted the following criteria for testing the magnitude of the weights on the steady terms. At the minimum point of the cost function, the different terms in the cost function are at the noise level of each term. The terms with temperature data, say, $(\hat{T}_{ijk} - T_{ijk}^{n=0})^2$, are equal on the average to the mean-square error in $\hat{T}_{ijk}$. As a result, the total contribution of these terms, after being multiplied by the weights (14) and summed over the volume of the ocean, is of order one. The same should hold for the steady-penalty terms as well. If the weights are chosen correctly, the total contribution of these terms in the cost function should be of order one (or at least of the same order as the temperature data terms, in case the cost function has been normalized by some multiplicative constant applied to all terms). The procedure of choosing the right weights for the steady terms is therefore iterative. We guess a value for the weights, minimize the cost function, and if the total contribution of these terms is not of the right order of magnitude, we modify the weights and repeat the procedure. Note that this procedure for calculating the weights on the steady penalties may not work when the model dy-

namics and the data are not consistent within the specified error bars, so that the terms in the cost function may be larger than order one. For an alternative approach to setting these weights, more appropriate when using real data, see Part II.

The use of diagonal weights, corresponding to an assumption that the errors are not correlated, is an unavoidable necessity due to the large size of the full error covariance matrices. A possible compromise, however, between the present simplification using diagonal weighting and the fully nondiagonal weighting could involve the specification of a correlation between the velocity and hydrography due to geostrophy only. Clearly, if the data errors are to be related mostly to the signal of mesoscale eddies present in the data, the dominantly geostrophic dynamics of the eddies suggests a relatively simple error correlation to be used in the weights of the velocity and hydrographic data terms in the cost function. In the present study, however, this approach is not taken, and this weighting strategy as well as a detailed examination of the consequences of using a completely uncorrelated error model are left to future studies.

b. *Weights: some particular limits*

It is instructive to try to understand the role of various terms in the cost function by examining some particular choices for the weights. By making some of the weights infinitely large or small, we recover various other approaches to ocean modeling as special cases of our optimization problem. Consider some of these special cases now.

1) NUMERICAL MODELS

Setting the weights on the surface forcing data terms and the steady-penalty terms to infinity and the weights on the temperature and salinity observations to zero, we recover the calculation of the steady-state general circulation using our model equations. With this choice of weights (and specifying rather than calculating the mixing coefficients), we in fact specify the surface forcing fields to be equal to the data, ignore the temperature and salinity data, and calculate the steady-state model solution using the optimization method. Ignoring problems of multiple minima points that may be encountered when searching for the minimum of the cost function, the solution of the optimization problem using this choice of weights should be identical to that obtained by specifying the surface forcing fields and mixing coefficients, and stepping the numerical model used in the optimization to a steady state. In fact, this approach provides an alternative to calculating the steady-state solution to our model equations, and this possibility was examined by Tziperman et al. (1992) using a simple QG model.

2) DIAGNOSTIC MODELS

Setting the weights on the temperature and salinity data terms and the surface forcing fields terms to infinity, and specifying the mixing coefficients, we recover the solution of a diagnostic model based on our model equations. In this case, the data are used as they are, without trying to obtain an optimal estimate for the hydrography or surface fields. As shall be seen below and in Part II, this approach is far less successful than the one in which the optimization is allowed to calculate an optimal estimate for the hydrography.

3) ROBUST DIAGNOSTIC MODELS

Specifying the mixing coefficients and setting the weights on the surface forcing fields to infinity, while leaving the weights on the T, S data terms and the steady penalty terms finite, we obtain an optimization problem that closely resembles the robust diagnostic approach of Sarmiento and Bryan (1982). In this case, the final solution of the optimization may differ both from the original data values for the hydrography and from the exact steady-state solution to the model equations. The additional terms added to the tracer equations in a robust diagnostic model have the same effect as the above choice of weights: the solution tends to be close, yet not necessarily equal, to the data, and the original tracer equations (without the restoring terms) are nearly, but not exactly, at a steady state when the final solution is found. In Part II the close relation between the robust diagnostic method and the present approach is demonstrated by using both with the same North Atlantic data.

The fact that these various approaches can all be recovered as special cases of the optimization method used here demonstrates the power and generality of the method, and its potential value to studies of the oceanic general circulation.

c. *Adjoint model*

The computational problem is to find the minimum of the cost function. We use a descent algorithm requiring the gradient of the cost function, which is provided by a so-called adjoint model. Like the model that has been obtained by modifying the GFDL PE model, the adjoint has also been obtained by modifying the adjoint code developed for the GFDL model at the Atlantic Oceanographic and Meteorological Laboratory of NOAA at Miami (Long et al. 1989). There is no need to give the details here, as the Lagrange-multiplier procedure has already been described several times (Thacker and Long 1988; Long and Thacker 1989; and in particular Tziperman and Thacker 1989), where the problem of analyzing general circulation data with the aid of a steady model is discussed in detail using a QG model as an example. An important point, however, is that an enormous effort was required to

construct the adjoint for a GCM of this complexity. Furthermore, any modification of the model requires corresponding modification of the adjoint.

d. *Optimization algorithm*

The optimization procedure is as follows: start with first-guess values for the control parameters, compute the cost function using the model, compute the gradient using the adjoint model, find improved values for the inputs using a conjugate-gradient descent algorithm, and repeat until the cost function is minimized. The conjugate-gradient algorithm incorporated diagonal preconditioning as described in section 4.8.5.2 (preconditioned conjugate-gradient nonlinear functions) of Gill et al. (1981). Using the gradient provided by the adjoint code, the descent direction was calculated using equations 4.88–4.89 from Gill et al., which are recommended for use with nonlinear functions. The line-search algorithm used to find the minimum of the cost function along the descent direction is that of NAG routine E04BBF (Numerical Algorithms Group 1984), which employs a safeguard cubic interpolation algorithm. The line search is stopped once an approximate minimum is found, based on inexact line search strategy [Gill et al. (1981), Eqs. (4.7), (4.8)]. This inexact line search strategy was found to be much more efficient than performing exact line searches at every descent iteration. The inherent nonlinearity of the cost function with respect to the different unknowns made it necessary to use this elaborate line search algorithm rather than the simpler procedure used by Derber (1985) and Long and Thacker (1989).

e. *Advantages of the simplified GCM*

The reasons for choosing the simplified model for this study rather than the full PE model have to do with the fact that the former is simpler to handle in the optimization. Having described the optimization algorithm, we now wish to discuss the three main practical motivations for preferring this modified version over the more general original version. First, because the momentum equations are diagnostic, there are fewer initial conditions to be calculated by the optimization (only T, S, while in the full PE model the baroclinic velocities and streamfunction also need to be specified as initial conditions). Second, the linear momentum equations reduce the nonlinearity of the model. When the model equations are used as constraints in the cost function (via the steady-penalty terms), the reduced nonlinearity may be expected to make the minimization of the cost function less of a problem. Finally, the diagnostic momentum equations allow the use of much larger time steps than a primitive equation model. This may prove useful in future studies of time-dependent problems such as the annual cycle or the analysis of transient tracers in the ocean. With a single time step used here to estimate the steady penalties in the cost function, the size of the time step is immaterial, but the first two advantages are relevant to the problems approached here. Considering the lack of oceanographic experience with the application of the adjoint method to oceanic models, we preferred to sacrifice completeness of the PE model for the aforementioned advantages.

4. Examples

The computational examples presented here all involve simulated data that have been generated by the same numerical model that was used in their analysis. In some of the examples, the data were of the identical-twin type (model results were used as data, with no noise added), so successful analyses should recover exactly the model inputs used to generate the data. These examples demonstrate that the optimization approach utilizing the adjoint method for calculating the gradient of the cost function does indeed work with a model as complicated as a 3D oceanic GCM, and they illustrate the effects of the type and number of data on the efficiency of the optimization algorithm. In other examples, randomly generated noise has been added to the data, making an exact recovery of the inputs less likely. The noise makes the simulated data somewhat more realistic and the results more indicative of what might be expected from real oceanographic observations. The inverse problems illustrated in these examples are all defined by the cost function (13) for a particular set of control variables and for specified values for the weight coefficients. The computational examples are summarized in Table 1 and described below. They are roughly arranged from simple to complex. We begin with very simple inverse problems that could, in fact, be solved using simpler methodologies, and then proceed to more complex problems for which the adjoint method was essential. The first examples involve calculating surface fields (heat and salt fluxes, and then surface wind stress), and later we also attempt calculating optimal estimates for the interior temperature and salinity fields, making the problem inherently nonlinear. The final examples involve nonlinear optimizations in the presence of noise, serving as a link to Part II, in which North Atlantic data that are noisy and possibly even inconsistent with the model were analyzed.

The model basin for these examples is illustrated in Fig. 1, where surface land cells are masked out and the bathymetry contours indicate an idealized midoceanic ridge. This domain is represented by a grid of $25 \times 20 \times 6$ cells (some of which represent land) in the center of which temperature and salinity are computed, with velocities computed on cell boundaries. Each cell is $2° \times 2°$, with the basin situated between 14°N and 54°N. The thickness of the six layers are, from top to bottom: 50, 200, 500, 800, 1000, and 1200 m.

TABLE 1. A summary of the optimization runs discussed in the text, giving details of the data used in each inversion (separately indicating the data used in the cost function, and that used to specify some of the model parameters to be equal to the data values); whether noise was added to the data; what were the unknowns solved for by the optimization; and the figures with the results of each run. In all cases, the steady penalties for the temperature and salinity appear in the cost function. In the data and unknowns columns, T, S denote the temperature and salinity at all grid points; $\mathscr{H}$ and $E-P$ are the surface fluxes of heat and freshwater at all surface grid points; K_h, K_{v0} are the eddy coefficients for the horizontal and background vertical mixing, respectively; and $\tau = (\tau^x, \tau^y)$ denotes the two components of the wind-stress forcing.

When T, S were not treated as unknowns, they were set to the data values (whether noisy or not). When surface fluxes, wind, or eddy coefficients were not treated as unknowns, they were set to their "true" values (those used to obtain the steady-state solution that is used as data in the optimizations).

Run	Data terms in cost function	Specified parameters	Noisy data?	Calculated unknowns	Figures
A	—	τ, T, S	No	$\mathscr{H}, E-P, K_{v0}, K_h$	3
B	—	τ, T, S, K_{v0}, K_h	Yes	$\mathscr{H}, E-P$	5, 6
C	—	$\mathscr{H}, E-P, T, S$	No	τ	7
D	Surface (u, v)	$\mathscr{H}, E-P, T, S, K_{v0}, K_h$	No	τ	8
E	T, S	τ, K_{v0}, K_h	No	$T, S\mathscr{H}, E-P$	9
F	—	τ, T, S, K_{v0}, K_h	Yes	$\mathscr{H}, E-P$	—
G	T, S	τ, K_{v0}, K_h	Yes	$\mathscr{H}, E-P, T, S$	10
H	$T, S, \tau, \mathscr{H}, E-P$	—	Yes	$T, S, \tau, \mathscr{H}, E-P, K_{v0}, K_h$	11

Simulated data for these inverse problems were generated as follows. First, model inputs were specified: The background vertical mixing was set to $K_{v0} = 1.0$ cm^2 s^{-1}, horizontal mixing to 10^7 cm^2 s^{-1}; the model was forced with a zonal wind stress, surface heat, and water fluxes, all varying sinusoidally with latitude as shown in Fig. 1:

$$\mathscr{H}_{ij} = \cos(\pi(j-2)/(j_{\max}-4)) \times 30/(C_p \cos(\phi_j))$$

$$E - P_{ij} = \cos(\pi(j-2)/(j_{\max}-4)) \times 30/(\text{year} \times \cos(\phi_j))$$

$$\tau^x_{ij} = -\cos(\pi(j-2)/(j_{\max}-4))$$

$$\tau^y_{ij} = 0,$$

where C_p is the specific heat of seawater, $j_{\max} = 20$, and rows $j = 1, 19, 20$ are land cells, not shown in the figure. The heat flux $\mathscr{H}$ is of the order of 30 W m^{-2}, and the freshwater flux $E - P$ is of the order of 30 cm yr^{-1}. Using these inputs, the model was stepped forward in time until friction damped out transients and a steady state was obtained; about 1000 model years were required to spin up from rest using a time step of one model day. The steady-state temperature and salinity fields were saved to serve, with the possible addition of random noise, as simulated hydrographic observations. Figure 2 shows the steady-state solution for the temperature and velocity field at two selected levels. Next, assuming that various model inputs are unknown and that various datasets are available, we extracted the inputs from the simulated data using the optimization procedure outlined above.

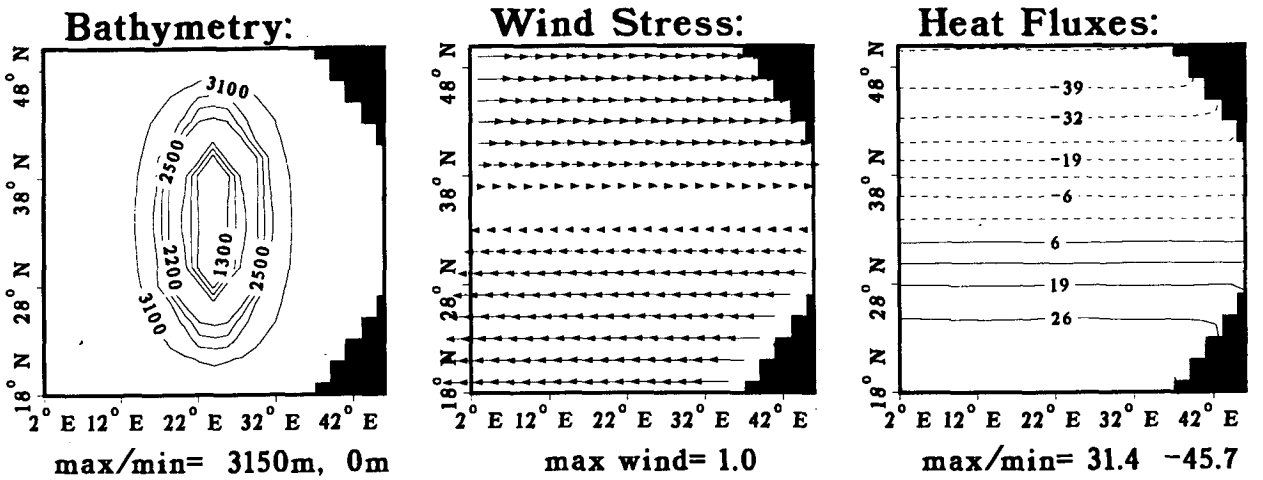

FIG. 1. Model geometry and bathymetry used for the simulations described in the text; surface flux of heat ($\mathscr{H}_{ij}$) and wind-stress field $\tau = (\tau^x, \tau^y)$ used to obtain the steady-state solution that was used as simulated observations.

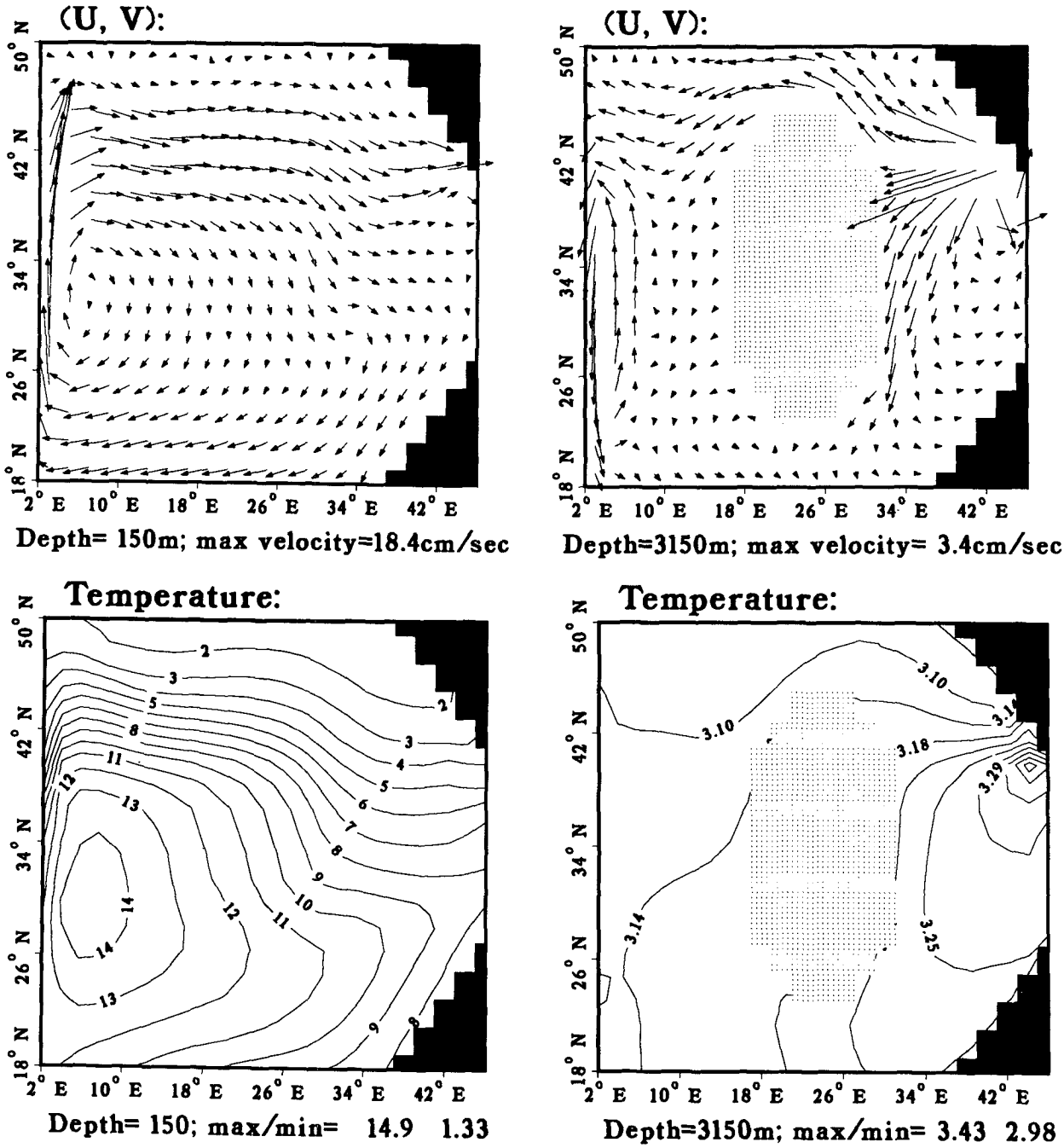

FIG. 2. Steady-state model temperature and velocity fields at two depths. Various combinations of these fields are used as data in the inversions presented in the text.

Consider first the problem of calculating the surface fluxes of heat and freshwater from hydrographic data, which is the subject of the first two examples.

(A) In the first example, surface fluxes of heat and moisture, as well as mixing coefficients, were treated as unknowns, while wind forcing, temperature, and salinity were assumed known and were fixed in the optimization. The wind-stress field was the same as that used in generating the simulated observations, and the temperature and salinity fields were set to their steady-state values. These fields (wind, temperature, and salinity) entered the optimization via the model equations relating the hydrographic fields at the two time levels. No surface-flux data were used, that is, $W^{\mathscr{F}} = 0$ and $W^{E-P} = 0$. Thus, the cost function simply

measured departures from the steady state. Furthermore, because the temperature and salinity fields were fixed, the only adjustable constraint in this optimization is the steadiness of the temperature and salinity equations at the surface level, while deeper levels have no effect on the optimization. In other words, the object of this inverse problem was to find the surface fluxes and mixing parameters leading to the steady balance for the observed surface temperature and salinity fields. To facilitate the analysis of this and the next examples, we explicitly write the steady penalties, so that the cost function may be written as

$$J(\mathscr{H}, E-P, K_{v0}, K_h) = \sum_{ij} [\bar{W}^T_{ij1}(\mathbf{u}\nabla T - K_h\nabla_H^2 T - [\mathscr{H} - \mathrm{K}_v T_z|_{\text{bottom}}]/\Delta z_1)^2 + \bar{W}^S_{ij1}(\mathbf{u}\nabla S - K_h\nabla_H^2 S - [\mathscr{H} - \mathrm{K}_v S_z|_{\text{bottom}}]/\Delta z_1)^2],$$

where $T_z|_{\text{bottom}}$ is the vertical temperature gradient at the bottom of the first model layer, and the sum is over all surface grid boxes.

To start the descent algorithm, the initial guesses for the fluxes were zero, and the initial guesses for the mixing coefficients were half their true values. Solving for these unknowns (about 25 times 20 surface grid locations times 2 functions, plus 2 mixing coefficients, corresponding to about 1000 unknowns) required only about 25 conjugate-gradient iterations, each including 1–4 runs of the forward and adjoint models. The accuracy of the calculated fluxes was better than 0.1%. The descent of the cost function as well as the distance of all unknowns from their true values as functions of the iteration number are shown in Fig. 3.

The success of the optimization in this case is not surprising. In fact, the heat fluxes could have been solved at every surface grid point by requiring the temperature and salinity to satisfy the steady equation. This can be done locally at every surface grid point, so that

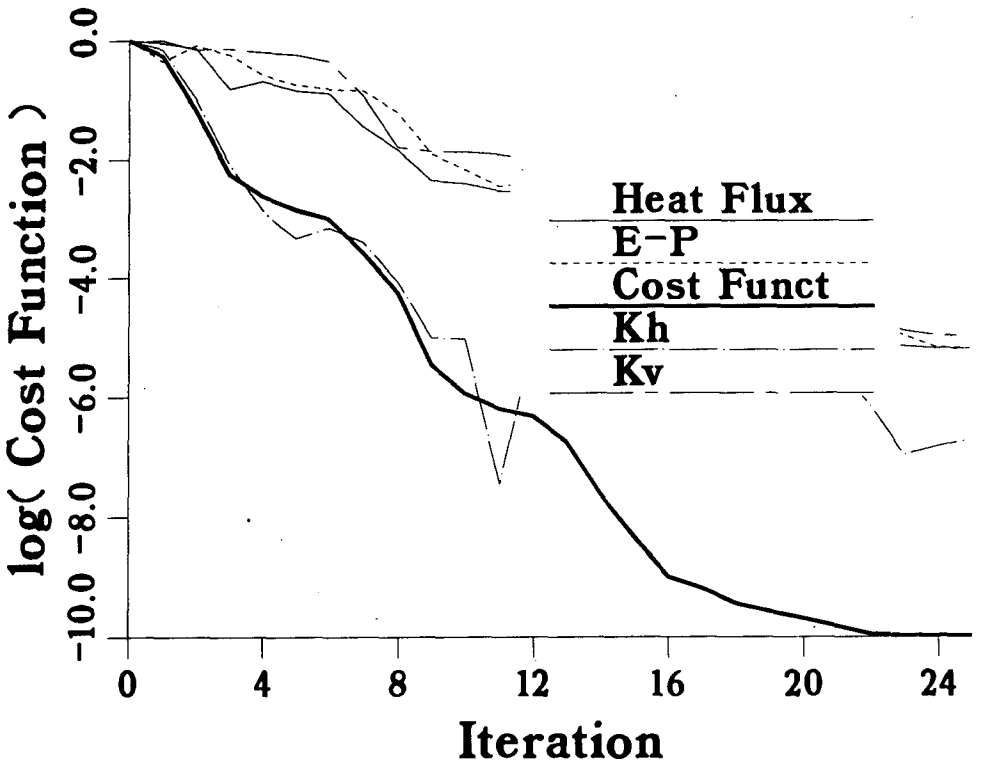

FIG. 3. Run A. Calculating tracer mixing coefficients and surface fluxes of heat and fresh water from perfect (identical twin) temperature and salinity data. Cost function and distance of model parameters from their true values are shown as functions of conjugate-gradient iteration number. The J denotes cost function normalized by its initial value. Curves denoted by H and $E-P$ are the distance between the calculated heat and freshwater fluxes and their true values, for example, $\Delta\mathscr{H} = [\Sigma_{ij}(\mathscr{H}_{ij}(\text{iteration}) - \mathscr{H}_{ij}(\text{correct}))^2]^{1/2}$. All plotted quantities are normalized by the initial values at the beginning of the minimization procedure. Similarly, K_h and K_v denote the absolute value of the difference between the mixing coefficients and their correct values, normalized by the correct value.

the conjugate-gradient minimization is not really necessary for calculating the surface fluxes alone. The addition of the mixing coefficients to the set of adjustable parameters does complicate the problem in making it nonlocal. But no difficulties are expected as a result of this because the two tracer equations for any interior grid box could be used to calculate the two mixing coefficients. It is useful to consider this simple case as our first example as a basis for comparison with later experiments, as well as a check that the gradient is accurately calculated by the adjoint. Next, consider the same inverse problem except that simulated noise is added to the temperature and salinity data.

First, a few words on the form of the random noise added to the simulated data in these experiments. There are two ways in which the optimization approach can be used with real hydrographic data. The first is to use the original data along ship tracks, and to include it in the cost function terms that require the model results at a given grid point to fit the observations near that point with some weighting based on the distance of the observations from the model grid point. In this case, one may also want to include in the cost function smoothing terms that prevent the noise in the data from affecting the calculated model inputs (Thacker 1989). The second and simpler strategy, which we simulate here and adopt in the study of the North Atlantic Ocean in Part II, is to first use some objective mapping procedure to map the original data into the model's grid, and only then use the gridded data in the optimization. When choosing the second strategy, we do not expect to find small-scale noise in the data, because it was smoothed by the objective mapping, but only larger-scale aliasing of the data due to the inability of the objective mapping to form fields that are both smooth and consistent with the dynamics. To simulate this type of noise in the data, we have chosen to add to the hydrographic fields noise of the form:

$$\text{noise}_{ijk} = A_k \sum_{l=1}^{4} R_l \sin(l\pi(i/i_{\max} + j/j_{\max}) + \pi k/4.0)), \quad (15)$$

where the R_l were calculated by a random number generator, and the amplitude of the noise at each vertical level k is controlled by the factor A_k (Fig. 4). The resulting noise is a large-scale, correlated aliasing of the data, roughly representing the aliasing one expects to find in objectively mapped oceanographic data. Similar expressions were used for the noise added to the 2D surface-forcing fields.

Consider now a similar inverse problem to that of (A), except that the mixing coefficients were not calculated and noise was added to the hydrographic data everywhere (but not to the surface forcing data).

(B) In this example, the control variables were the surface fluxes of heat and moisture. Temperature and salinity initial conditions were held in agreement with

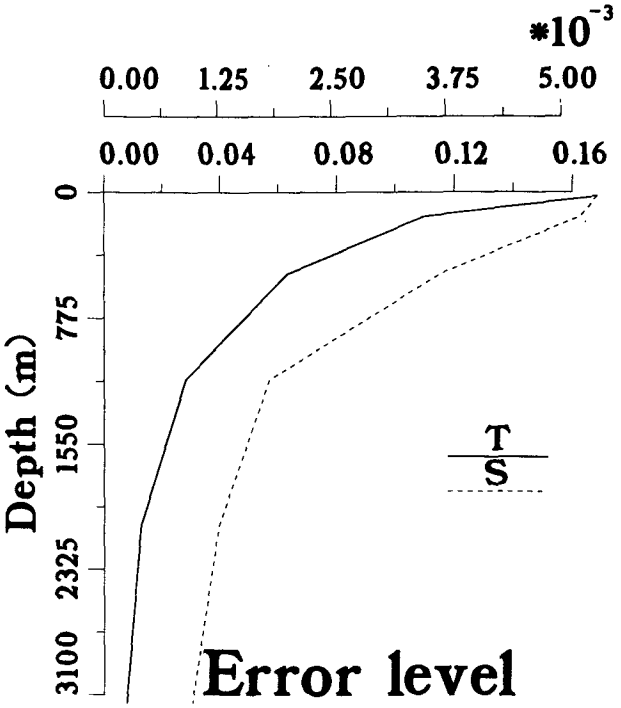

FIG. 4. The amplitude of the noise level added to the simulated temperature (lower horizontal axis) and salinity (upper axis) data, as a function of depth [see (15)].

the noisy data. The wind-stress field was also held fixed at noise-free data values, and the mixing coefficients were also the same as those used in generating the hydrographic data. Figure 5 shows the recovered surface fluxes. This solution is quite good in the southern part of the basin but badly aliased in the northern part. To understand this solution, note that, as in the previous example, the fluxes were actually calculated locally at each surface grid box in order to satisfy the steady balance for the temperature and salinity. The optimization had no way of improving the fit to steady state for the deeper grid boxes, but could achieve fully steady balance for the upper grid boxes by modifying the surface fluxes. This, of course, means that all errors in hydrographic data must be compensated for by modifying the surface fluxes. In the southern part of the basin the small errors in the temperature and salinity data were translated into relatively small errors in the solution for the fluxes. In the northern half of the basin, however, the error seems to have been amplified so that the resulting fluxes are badly aliased.

The reason for the large errors in the fluxes recovered in the northern half of the basin seems to be the presence of water-mass formation and strong vertical mixing in the northern part of the basin. Figure 6 shows the depth of convection in the model, that is, the region in which the vertical mixing coefficient as determined by the Richardson number parameterization (7) is larger than or equal to $K_{\max}$. This region lies in the

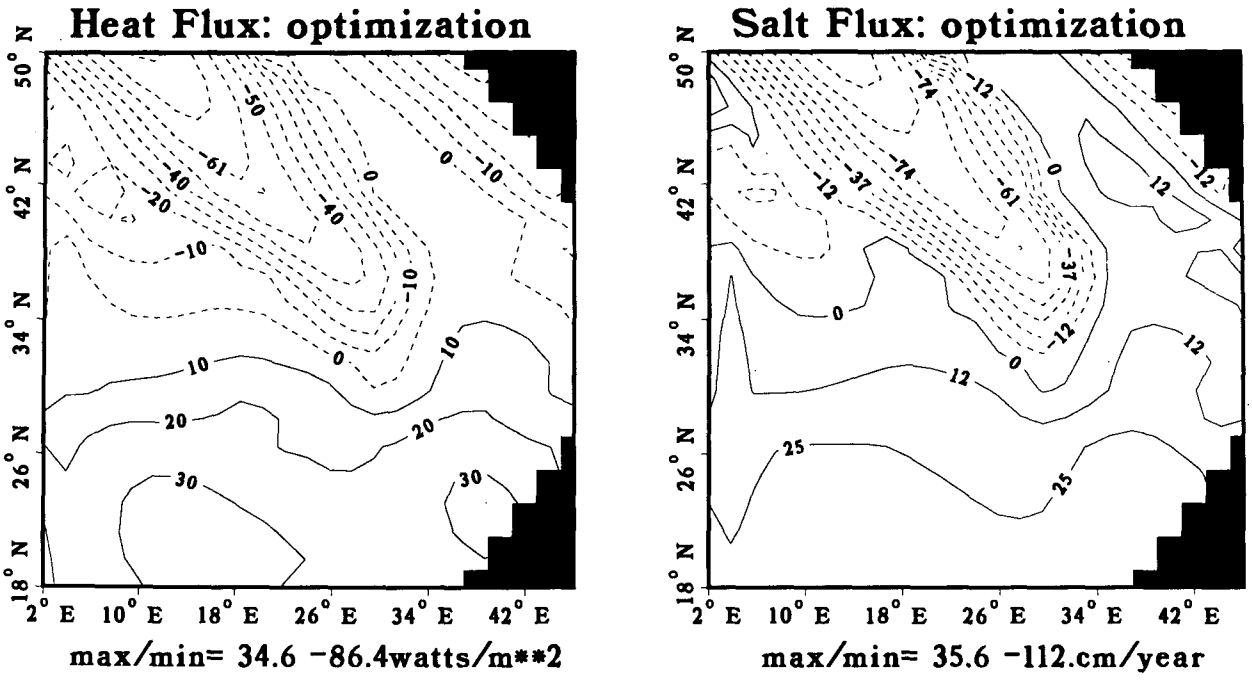

FIG. 5. Run B. Calculating surface fluxes of heat and $E - P$, from noisy temperature and salinity data. The final solution calculated by the optimization for the heat and salt fluxes.

northern half of the basin. Where strong mixing reaches the bottom, deep water is formed in the model. The errors in the hydrography result in errors to the vertical temperature gradient at the bottom of the first model layer, which appears in the steady penalties for the upper grid boxes (see the term $K_v T_z|_{\text{bottom}}$ in the cost function for run A). This error was strongly amplified when multiplied by the large vertical mixing coefficient K_v in the regions of strong vertical mixing. As the surface temperature and salinity are related to the heat and fresh fluxes via the steady balance appearing in the cost function for example (A), this amplified error must be balanced by the optimization by making large corrections to the surface fluxes. The small errors in the surface hydrography resulted, therefore, in large errors in the calculated surface fluxes.

Strong vertical mixing due to convective processes seems, in general, difficult to handle for the optimization. The noise amplification problem described above (i.e., the large errors in the solution for the surface fluxes due to relatively small errors in the hydrographic data) is not the only difficulty due to convective processes. Another possible problem is that the convective adjustment may cause sharp changes in the value and the gradient of the cost function as the Richardson number approaches the critical value of $\frac{1}{4}$. Such sharp changes deteriorate the performance of the conjugate-gradient algorithm and may prevent progress of the minimization toward the global minimum of the cost function. In preliminary simulations with the model described here, we have used a convection algorithm that mixes adjacent layers where the density is unstable until they become vertically uniform (Cox 1984). This is equivalent in a way to using a value of $K_{\max} = \infty$ in the parameterization (7) and causes even sharper changes in the cost function as the density field approaches an unstable regime. With this convection parameterization the optimization was unable to calculate the correct wind forcing even from identical twin data. The parameterization (7) is characterized by a smoother behavior of the cost function, but as demonstrated above, regions of convection still pose a difficulty as far as the optimization is concerned.

In order to avoid the problems caused by the regions of strong mixing and water-mass convection in the following simulations with noisy data, we added noise only to the data in the southern half of the basin. All quantities in the northern half were set to their true values and are not treated as unknowns in the optimization. This allowed us to concentrate on some other issues relevant to steady inverse problems involving complex GCMs.

The next two inverse problems concern the calculation of surface wind stress from hydrographic data. These problems still involve the calculation of 2D surface fields while fixing the values of the 3D temperature and salinity, so that they are simpler than the fuller problems discussed later. Yet these inverse problems present new difficulties for the optimization, as the wind stress is related to the hydrographic data less directly than the heat and freshwater fluxes. As will be explained, the optimization required the full 3D data

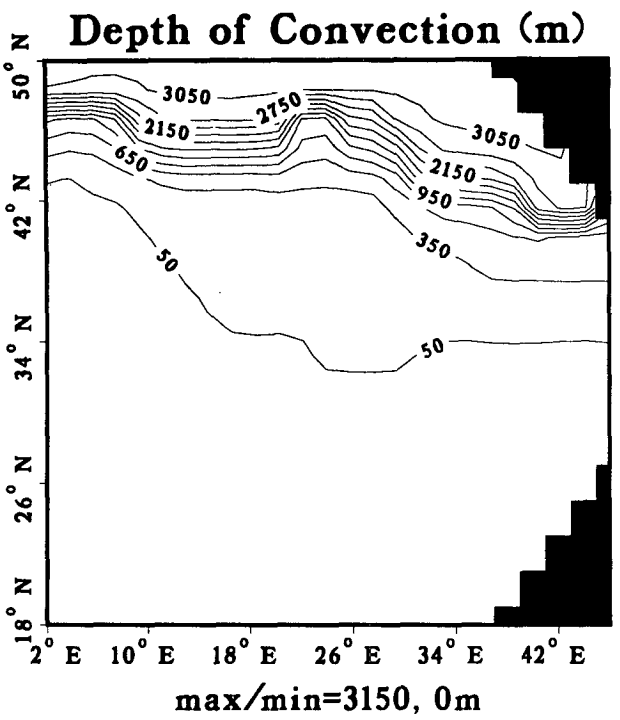

FIG. 6. Run B. Calculating surface fluxes of heat and $E - P$, from noisy temperature and salinity data. The depth of convection regions in the model at steady state (see text).

fields in order to calculate the surface wind stress, and the calculation was neither local nor limited to the surface layer as in the previous two examples.

(C) In this example, the wind stress was the only input to be estimated. Temperature, salinity, mixing coefficients, and surface fluxes were all set to their true values. The wind stress was to be estimated from the hydrographic data using the numerical model with the specified fluxes and mixing parameters, so no wind-stress data were used, that is, $W^\tau = 0$. Again, the cost function simply measured departures from steady state, and the objective was to find the wind forcing consistent with the specified hydrographic data, surface fluxes, and mixing coefficients. The cost function is therefore

$$J(\tau^x, \tau^y) = \sum_{i,j,k} [\bar{W}^T_{ijk}(T_{t,ijk})^2 + \bar{W}^S_{ijk}(S_{t,ijk})^2].$$

A first guess of zero stress everywhere was used to initiate the descent algorithm. The optimization was able to converge to the correct solution for the wind-stress field, yet many more iterations were needed than in the previous examples (Fig. 7), indicating that the problem is ill conditioned, or, in other words, that the temperature and salinity data together with the surface-flux data were just barely sufficient for calculating the wind forcing. To see why this is the case, note first that the calculation of the wind stress involves two unknown 2D fields (x and y components of the wind stress). We therefore expect that a successful calculation of these fields requires the total number of independent data to be at least that of two 2D fields. Consider next the flow of information in the optimization from the data to the unknown wind-stress fields. The wind stress does not directly enter the tracer equations. Its effect on these equations is through the influence of the wind field on the velocity field. For the inverse problem this implies that, in order to calculate the wind stress from the steady tracer constraints, it should be possible to infer the velocity field from the tracer distributions by searching for the velocity field that would bring the tracer balances to a steady state. Only then can the optimization calculate the wind stress that results in the velocity field required by the steady tracer constraints. As the wind stress enters directly the equations for the upper-layer velocities, it seems that if the optimization can infer the two 2D fields of the u and v velocities at the surface layer, it should be able to easily calculate the wind stress from this information.

In principle, it seems that there should be no difficulties in inferring the surface velocities from the temperature and salinity constraints. The steady-penalty constraints for the temperature and salinity at the surface should provide the two needed independent 2D sources of information allowing the determination of the u and v surface velocities. In the specific case considered here, however, the temperature and salinity do not provide independent information because their boundary conditions are similar (see specification of

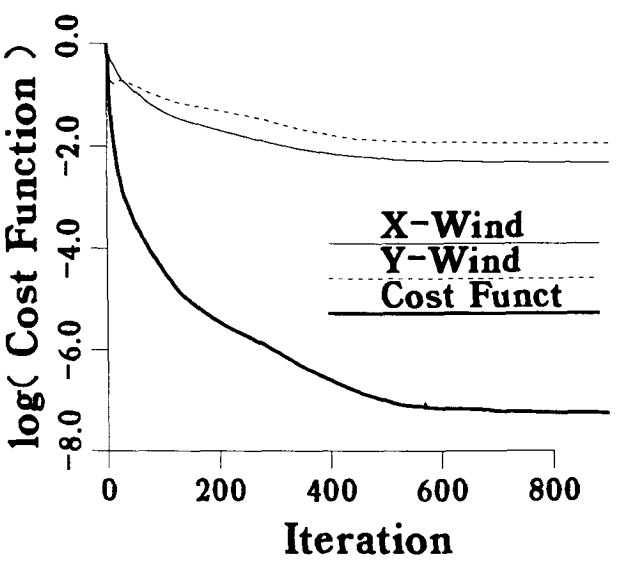

FIG. 7. Run C. Calculating wind forcing from perfect (identical-twin) temperature and salinity data. As in Fig. 3, with X-Wind and Y-Wind denoting the distance between the wind-stress forcing calculated by the optimization and the correct ones (in the x, y directions, respectively).

the boundary conditions at the beginning of this section), and therefore their steady-state distributions are similar. There is still sufficient information to calculate the wind stress, because the 3D steady penalties for the temperature provide more data than the two unknown 2D wind-stress components. But the direct link between surface properties, surface velocities, and surface wind stress cannot be utilized by the optimization. Rather than using the surface T, S constraints to determine the surface velocities and from that determine the wind stress, the optimization must use the 3D steady-penalty information to infer two 2D wind-stress components at the surface. This longer path of information from the data to the unknown parameters resulted in bad conditioning and therefore relatively slow convergence. To further support this interpretation of the results, we performed the next experiment, in which direct velocity information was provided, and tried to calculate the wind stress using these additional data.

(D) In this experiment, the set of model-generated observations was enlarged to include surface velocities. A term was added to the cost function requiring the model velocity field at the surface to be consistent with the observations,

$$J(\tau^x, \tau^y) = \sum_{i,j,k} [\bar{W}^T_{ijk}(T_{t,ijk})^2 + \bar{W}^S_{ijk}(S_{t,ijk})^2] + \sum_{i,j} [W^U_{ij1}(\hat{u}_{ij1} - u_{ij1})^2 + W^V_{ij1}(\hat{v}_{ij1} - v_{ij1})^2].$$

Convergence to correct wind forcing was rapid now, within less than 100 iterations (Fig. 8).

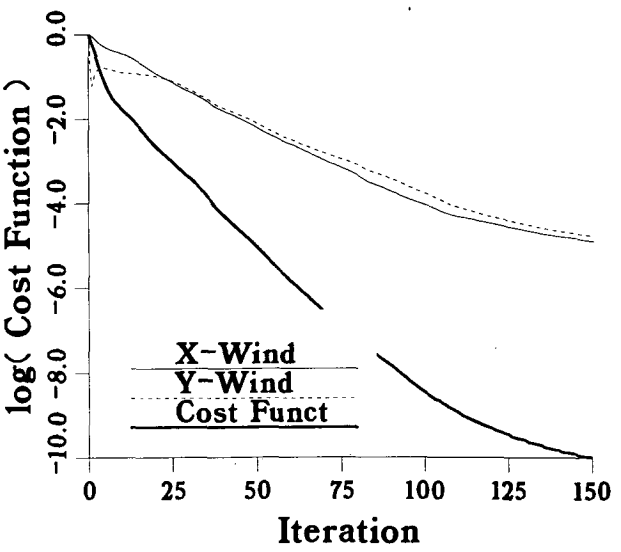

FIG. 8. Run D. Calculating wind forcing from perfect (identical twin) temperature, salinity, and surface-velocity data. Curves are as in Fig. 3. Note that the convergence to the optimal solution requires fewer iterations, and the accuracy of the solution is better than without the surface-velocity measurements (run C, Fig. 7).

The improvement in the convergence to the correct wind forcing as a result of adding surface velocity observations (runs C and D) confirms our suspicion that the slow convergence of the previous example resulted from the inability of the temperature and salinity fields to provide independent information allowing the direct calculation of the surface velocities.

It is important to note that the difficulties encountered in calculating the wind stress from hydrographic data may also be found when analyzing real oceanographic data, where salinity and temperature do not have the same boundary conditions. In regions of strong horizontal advection, for example, both the temperature and the salinity equations are dominated by the horizontal advection terms, with vertical velocities, mixing processes, and surface fluxes playing a secondary role. The zero-order equations for the temperature and salinity are then $J(\psi, T) \approx 0$, and $J(\psi, S) \approx 0$, where the Jacobian with the streamfunction represents the advection by the horizontal velocities. This also implies $J(T, S) \approx 0$, or, in other words, that the temperature and salinity in these regions are not independent of each other. In such cases, as in our example (C), the surface temperature and salinity cannot be used to extract the surface velocities, resulting in a difficulty to calculate surface wind stress. It seems, therefore, that one might generally need more than hydrographic data to calculate the wind-stress forcing.

Having explored, at least partially, the problem of calculating surface forcings from interior data, we now proceed to a different class of inverse problems—those involving the calculation of optimal estimates for the temperature and salinity data as well as estimating other model parameters.

(E) Consider first an identical-twin data experiment in which we calculated surface fluxes from T, S data while allowing the temperature and salinity fields to vary in the optimization. Unlike the situation in example (A), the hydrographic data terms of the cost function were not identically zero and played a significant role in the calculation. In addition to significantly increasing the number of unknowns, we have also made the problem inherently nonlinear, and therefore potentially far more difficult than before. The cost function for these computations, including the data and steady penalties for the temperature and salinity fields, is

$$J(\mathscr{H}, E-P, T, S) = \sum_{i,j,k} [\bar{W}^T_{ijk}(T_{t,ijk})^2 + \bar{W}^S_{ijk}(S_{t,ijk})^2] + \sum_{i,j,k} [W^T_{ijk}(\hat{T}_{ijk} - T^{n=0}_{ijk})^2 + W^S_{ijk}(\hat{S}_{ijk} - S^{n=0}_{ijk})^2].$$

Note (Fig. 9) that although the initial guesses for T and S were the same as the true solution, convergence was still much slower than in run A. During the first iteration, the optimization had modified the temper-

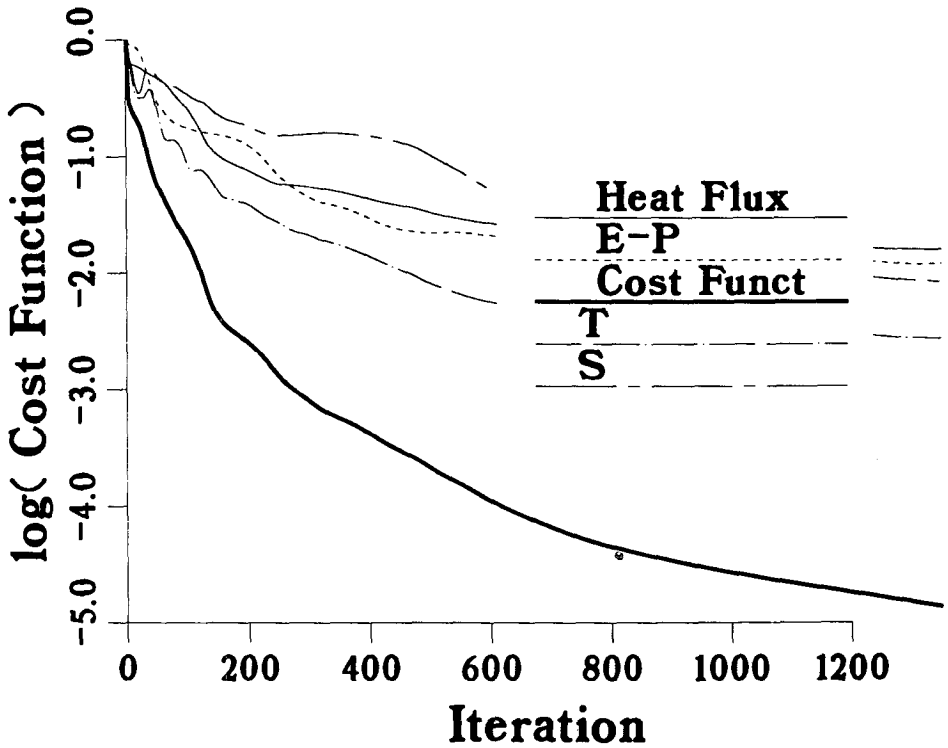

FIG. 9. Run E. Repeating the calculation of heat fluxes and $E - P$ from identical-twin data, as in run A, except that now temperature and salinity are also treated as unknowns that vary in the optimization. The initial guess for the temperature and salinity is the true steady-state solution, but at the first iteration the guess calculated by the conjugate gradient for T and S is away from the true solution. The estimates for the temperature and salinity fields are improved again during the optimization. Note that convergence to the final solution is much slower than in run (A), although the correct solution is still calculated for all fields.

ature and salinity fields, so that they were no longer at the data values and had to be corrected together with the surface fluxes. This comparison between the convergence rate of two different inverse problems raises the question of what criteria should be used for determining how well the optimization performs. With identical-twin data we have, of course, the advantage of knowing if the solution found by the optimization is correct or not. But another important factor is the conditioning number of the problem. If the conditioning number is much larger than one, the problem is badly conditioned, indicating that convergence will be slow, small errors in the data will be amplified, and the data used may not be appropriate for calculating the desired unknown parameters. Without calculating the conditioning number directly, our indications for how well conditioned a given problem is, come from examining the convergence rate and the amplification of noise. In example (A), with about 1000 unknowns (surface heat and freshwater fluxes), convergence (measured as the number of iterations needed to reduce the cost function by 5 orders of magnitude) was within 10 iterations; in example (D), when calculating the surface wind stress (again about 1000 unknowns) from surface velocities, convergence was within about 50 iterations. It seems that a well-conditioned problem involving surface forcings required a number of iterations, that is, of the order of no more than $1/20$ of the number of unknowns. The seemingly poorly conditioned problem of calculating the surface wind stress from hydrographic data alone required about 200 iterations for 1000 unknowns, or a ratio of 1:5 between number of unknowns and number of iterations. For the present problem, the number of unknowns is of the order of 7000 (surface fluxes plus temperature and salinity), and the solution is found within about 1200 iterations. The ratio between the number of unknowns and iterations is again about 1:5, indicating that the problem might be ill conditioned. The conditioning of the inverse problem is an important issue, and we will return to it later after examining the results of the experiments with noisy data. At this stage, however, it is clearly seen that the rate of convergence (or equivalently, the conditioning of the problem) depends on

both the type and number of data used to recover the model inputs.

Having examined the nonlinear problem in the identical-twin data limit, we now complicate the problem by adding simulated noise to the identical-twin data. Some difficulties are expected, as the problem without the added noise seemed to be somewhat ill conditioned, and this may imply a severe noise amplification.

(F–G) Consider, then, the same inverse problem as in the previous example: temperature and salinity data were used to calculate surface fluxes of heat and freshwater, with wind stress and mixing coefficients fixed as before, but this time, noise was added to the data. While calculating the fluxes, we also wished to obtain an optimal estimate for the noisy hydrography itself and to examine the effect of this added degree of freedom on the noise amplification problem seen in experiment B. For this purpose, two experiments were performed in which the surface fluxes of heat and fresh water in the southern half of the basin are calculated from noisy T and S data. This was first done with the temperature and salinity fixed to the values of the simulated noisy data (run F), and then allowing them to vary in the optimization (run G). In the second case (G), we tried to compute, therefore, optimal estimates for both the surface fluxes and the hydrographic data. (Run F actually repeats run B except that noise was added in run F only in the southern half of the basin.) Because the hydrography was allowed to vary in optimization (G), we expect to obtain better results than by fixing the hydrography and varying only the surface fluxes (F). In the latter case, we have seen (run B) that all the errors are projected into the surface fluxes, resulting in a badly aliased solution for them. With the hydrography as a control variable as well, the noise should be somehow distributed between the fluxes and hydrography, hopefully giving better estimates for both.

For the comparison between the results of runs (F) and (G), the error in the calculated fluxes is measured by the rms difference between the true fluxes and their values as calculated by the optimization, divided by the rms value of the fields. When the hydrography was also varied (G), the error in the fluxes is indeed somewhat smaller than when only the fluxes were calculated (run F): $\mathrm{rms}(\mathscr{H} - \hat{\mathscr{H}}, E - P - \hat{E} - \hat{P})$ = (19.63%, 21.51%) for run F and (17.07%, 20.30%) for run G. While the error in the value of the surface fluxes is of the same order in both runs, the second optimization did succeed in improving the noisy T, S data and reducing the rms of $(T - \hat{T}, S - \hat{S})$ to (59.6%, 64.1%) of the original value of the noisy data before the optimization (Fig. 10a).

The improvements to the air–sea flux data were found to be quite sensitive to the level of noise in the hydrographic data, even away from the regions of convection. The quite low noise level in the simulated T, S data (Fig. 4) that were used in the above simulations resulted in errors of the order of 20% in the calculated fluxes. Reducing the amplitude of the error in the hydrographic data also reduced the errors in the fluxes calculated from these data. When using real hydrographic data, however, errors can be expected to be at least as large as those shown in Fig. 4. In fact, real oceanographic data may also be expected to be inconsistent with the model, so that the noise amplification may be expected to be even worse than found here. This noise amplification is possibly a result of the ill conditioning of the optimization, as observed in the identical-twin experiment (E). The conditioning of the optimization is further discussed below and is analyzed in detail in Part II of this work.

We conclude from this pair of experiments that treating all model inputs, including the temperature and salinity fields, as unknowns to be calculated by the optimization can result in a better estimate for all observed fields. The improvement is significant for the temperature and salinity, but fairly negligible for the surface fluxes, perhaps due to the ill-conditioning problem. The hydrographic data must be taken as it is by linear inverse methods in spite of the obvious fact that it contains errors and inconsistencies with the dynamics. Obtaining an optimal estimate for the hydrographic data itself should therefore be an important part of the inverse calculation, and this in fact is done by nonlinear inverse methods (Mercier 1989). The allowed complexity of the dynamics and the higher resolution of the GCM used for the analysis, however, are superior to what has been practical with other nonlinear inverse methods.

As a final example, which will serve to link these experiments with simulated data to those with real oceanographic data discussed in Part II, a problem of the type encountered in real oceanographic applications is considered. Noisy data for the hydrography, surface fluxes, and wind stress were used together with our GCM in order to try to obtain an optimal estimate for the counterparts to these data, as well as for the two mixing coefficients.

(H) Figure 11a shows the descent of the cost function as a function of the iteration number as well as the distance between the various inputs calculated by the optimization and their true value. Figures 11b–d show the data versus the optimal solution for the surface forcing fields. Tables 2 and 3 summarize the results of the optimization and the improvement (if any) in all model inputs relative to the initial data for these inputs. Figure 11e shows the deviation from steady state $(T_{ijk}^{n=1} - T_{ijk}^{n=0}$, for $k = 1)$.

As could have been anticipated from the previous experiments, the improvement to the air–sea flux data and the wind data was not large at the level of noise we have added to the temperature and salinity data. Overall, the optimization did improve the hydrographic data, and to some extent also the surface forcing fields. Note (Table 3) that the final solution is characterized

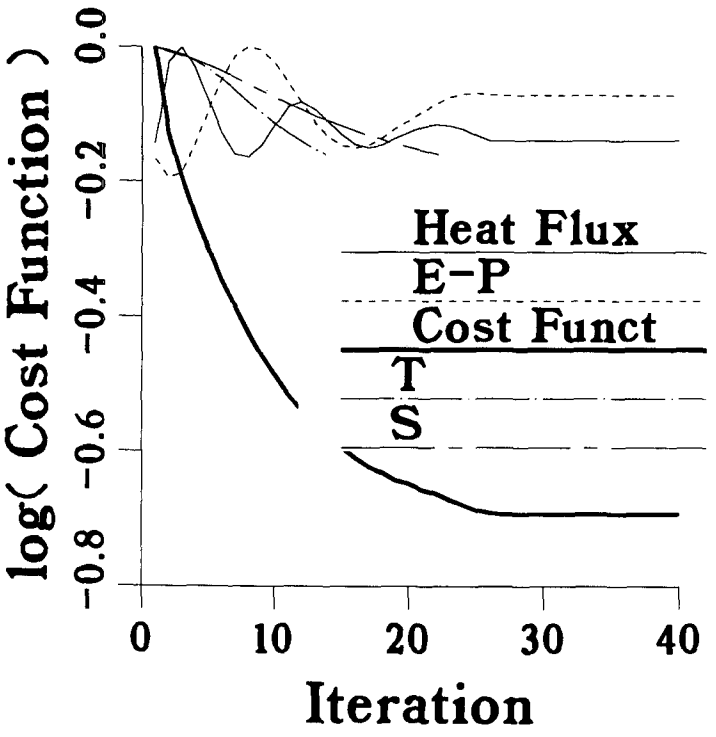

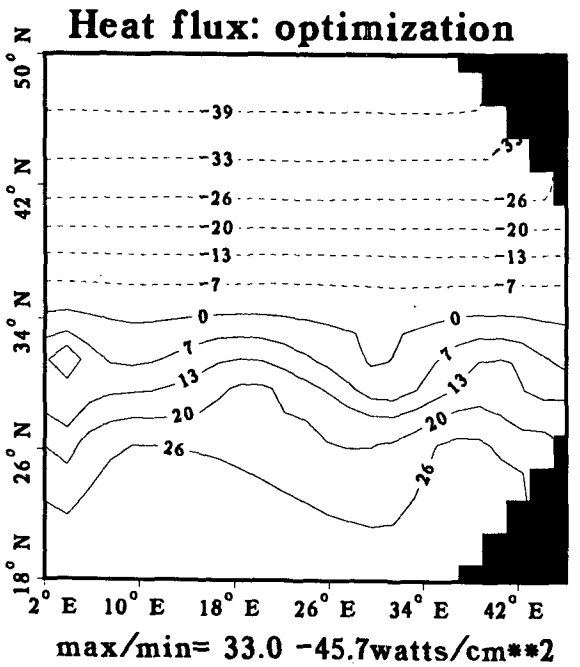

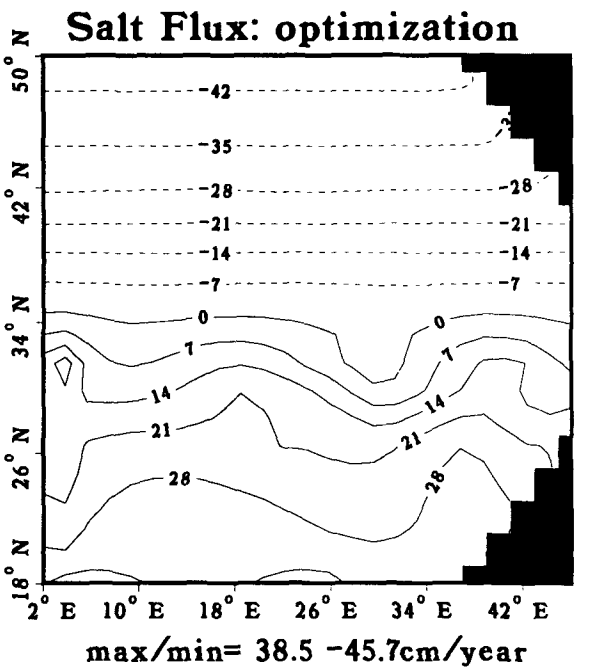

FIG. 10. Run G. Calculating surface fluxes of heat and $E - P$ from noisy temperature and salinity data, while also calculating an optimal value of the temperature and salinity fields. (a) Convergence of cost function as a function of iteration and the distance between the calculated fluxes and their true values; also showing the distance between the true T, S and the optimization solution. Note that this distance decreases as the optimization proceeds, meaning that the optimization is able to improve the noisy temperature and salinity data. (b) Final solution for the heat and freshwater fluxes.

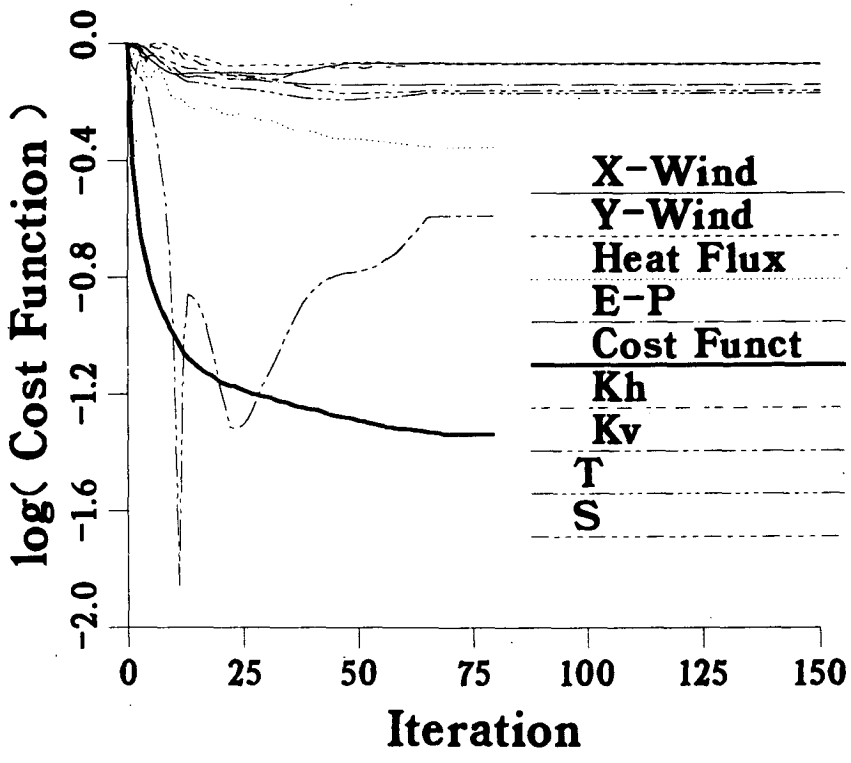

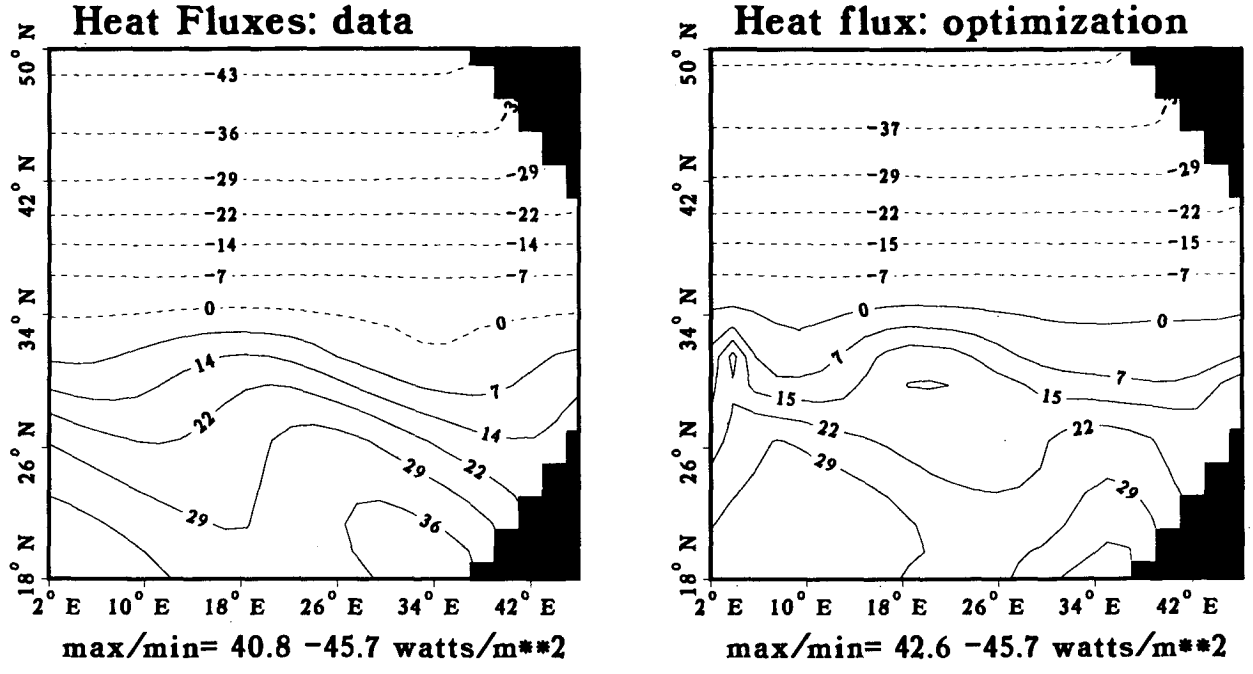

FIG. 11. Run H. Using noisy data of temperature, salinity, wind, and heat and freshwater fluxes to calculate an optimal estimate for all of these quantities, as well as optimal estimates for the tracer mixing coefficients. (a) Convergence of cost function and distance to true parameters as a function of iteration number. (b) Run H. Optimal solution for heat fluxes and the noisy data.

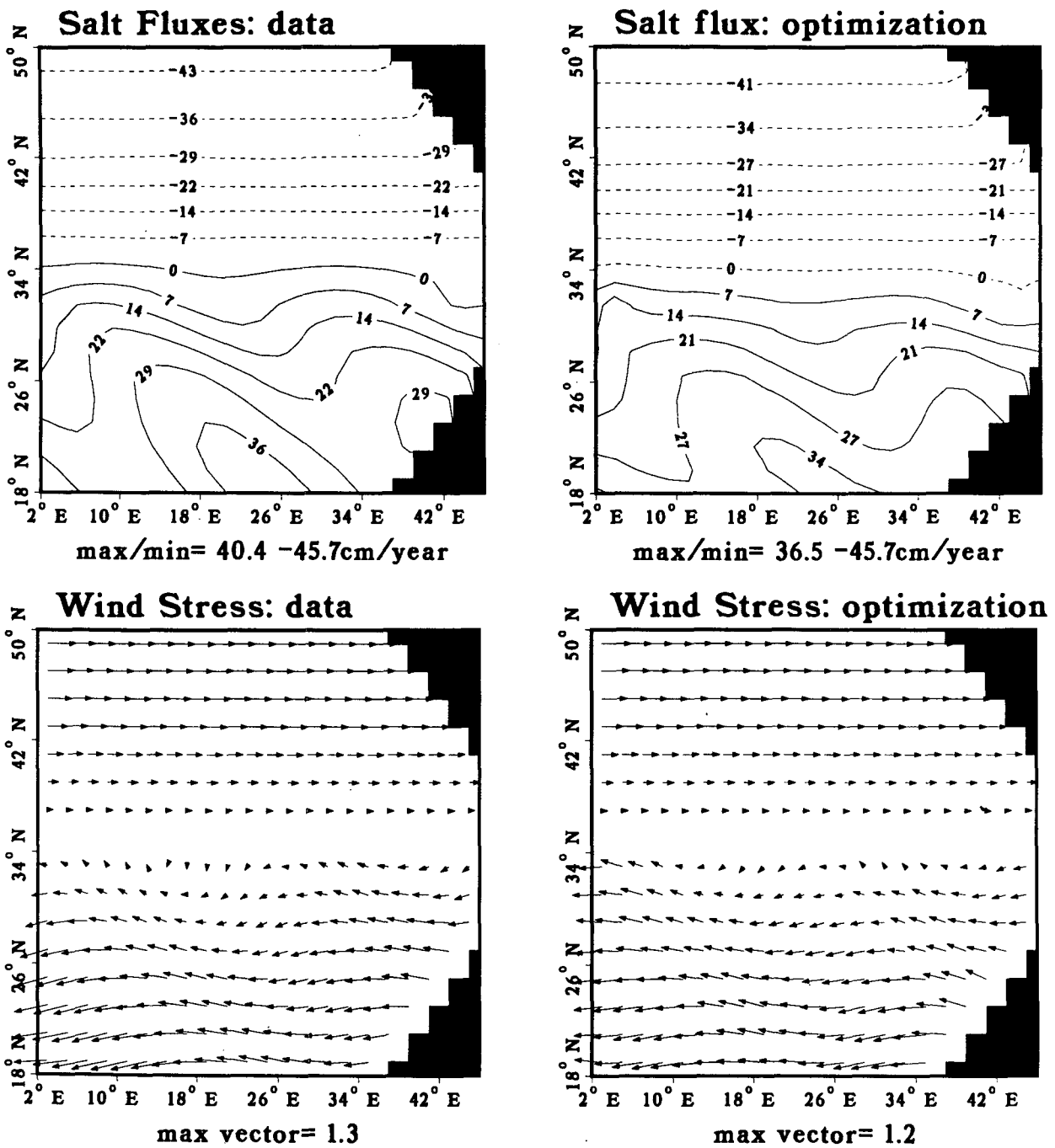

FIG. 11. (c) Run H. Optimal solution for salt fluxes ($E - P$) and the noisy data.
(d) Run H. Optimal solution for the wind forcing and the noisy data.

by residuals of the steady penalties and misfit to the hydrographic data that are of the same order of magnitude. This means that the optimization was able to balance between deviations from the steady penalties in the cost function and the penalties on deviations from the hydrographic data. The residuals of the terms measuring misfit to surface forcing data, on the other hand, are significantly smaller. This may mean that our solution does not balance the deviation from the surface forcing data with the deviation from the other data used in the cost function. As a result, this solution may not be the desired optimal solution for the surface fluxes. In Part II, it will be seen that the optimization has similar difficulties in balancing the residuals of the

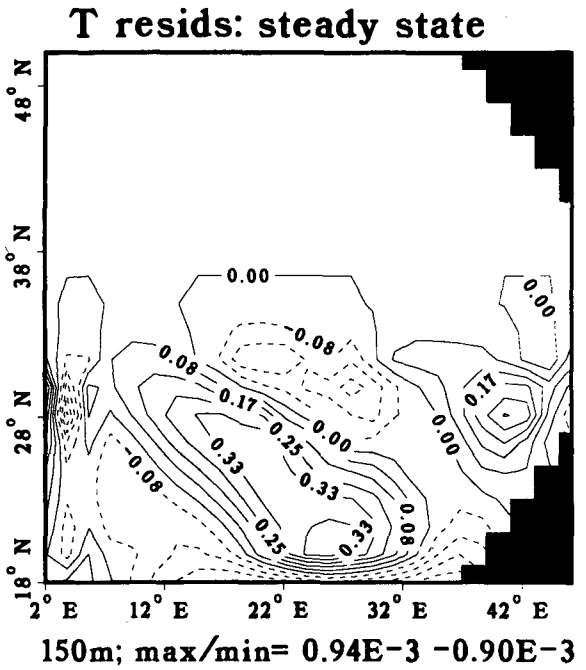

FIG. 11. (e) Run H. Deviation of the optimal solution for the surface temperature from steady state (T_i).

different terms in the cost function when applied to real North Atlantic data. This imbalance of terms in the cost function is further discussed and interpreted in Part II. Finally, we note that the vertical mixing coefficient calculated by the optimization was a better estimate to the true solution than the horizontal mixing coefficient. This seemed a consistent pattern in various additional simulations made in this study. With no error information about the calculated parameters, at this stage, this is taken to indicate that the error bars for the horizontal mixing coefficient are probably larger.

Thacker (1989) and Tziperman and Thacker (1989) showed that error and even resolution information can be obtained from the Hessian matrix (second derivatives of the cost function with respect to the model inputs). Tziperman and Thacker also proposed using a lower-resolution model for calculating the error information than that used for the optimization itself. Even with reduced resolution, however, the Hessian for an oceanic GCM such as we use here is enormous. It is an advantage of the adjoint method that the error covariance matrix need not be calculated as part of the solution procedure, which allows dealing with the very large optimization problems in which we are interested. Still, a feasible way of obtaining error information on the calculated model parameters is clearly needed.

The sensitivity to noise in the observations found in the noisy data experiments, and expressed in the lack of improvement in the model inputs when the noise level is increased above the low noise level of run H, may be due to two different problems. The first possibility, discussed earlier, is that the inverse problem is ill conditioned, resulting in noise amplification in the calculated parameters. The other possibility is that, due to the inherently nonlinear nature of the problem, there are multiple local minima of the cost function. The solution of run H may therefore not be the optimal solution corresponding to the global minimum of the cost function, but only a local minimum into which the conjugate gradient optimization converged. The conjugate-gradient minimization algorithm has no way of distinguishing local minima from the global minimum, making it possible, at least in principle, that our solution is such a local minimum.

It is important to realize that with the very large number of parameters calculated here, it is impossible to examine the way the cost function changes in all directions in parameter space. There is no practical and definite way, therefore, of finding out if the inability to further improve the model parameters is due to a stalling of the optimization resulting from bad conditioning, or due to local minima of the cost function. When exploring this question, the use of noisy identical-twin data offers no advantage over using real

TABLE 2. A summary of the results of the optimization involving all model inputs and using simulated noisy data (run *H* in Table 1). The subscript "true" refers to the value of the parameters with no simulated noise added.

Variable	Noisy data	Optimal solution	True value
K_{v0}	0.5*	1.13	1.0
K_h	0.53×10^7 *	0.53×10^7	1.0×10^7
rms($\mathscr{H} - \mathscr{H}_{true}$)/rms $\mathscr{H}$	0.2320	0.2235	
rms(E–$P - E$–P_{true})/rms E–P	0.2321	0.1677	
rms($\tau^x - \tau^x_{true}$)/rms τ^x	0.2059	0.1753	
rms($\tau^y - \tau^y_{true}$)/rms τ^x	0.2047	0.1794	
rms[$(T - T_{true}) \times \sqrt{W_k^T}$]**	130.9	89.31	
rms[$(S - S_{true}) \times \sqrt{W_k^S}$]**	113.8	78.75	

* The value specified for the mixing coefficients in the "noisy data" column is simply the initial guess for the coefficients. No data for these coefficients was used in the cost function.

** W_k^T and W_k^S are the weights (14) for the temperature and salinity data terms in the cost function.

TABLE 3. The different contributions to the cost function before and after the optimization of run H. The value J is the total cost function; the columns marked $\Delta(\ )$ give the contribution of various terms in the cost function (13). For example, for the temperature field, the term in the cost function measuring the deviation from the data is

$$\Delta T = \sum_{i,j,k} [W^T_{ijk}(\hat{T}_{ijk} - T_{ijk})^2].$$

The last column gives the combined contribution of all surface forcing terms in the cost function.

	J	ΔT	ΔS	ΔT_t	ΔS_t	$\Delta_T + \Delta H + \Delta(E - P)$
Before	1.15	0.	0.	.913	.240	0.
After	.0527	.0106	.0078	.0147	.0148	.0048

oceanographic data. On the other hand, we feel that important experience with real oceanographic problems may be gained by going at this stage to real data. For this reason, Part II, dealing with the questions of conditioning and local minima, is based on the analysis of real North Atlantic data, using the same model and methodology used here.

5. Conclusions

An important goal of physical oceanography is to combine available oceanographic data with realistic OGCMs in order to study the physics of the general circulation. This, however, poses a most complex large-scale computational problem that cannot be handled by standard methods and requires the use of more efficient mathematical procedures. In this work, we have used a GCM and simulated data to examine the possibility of formulating meaningful and solvable inverse problems involving a full-sized OGCM using an optimization approach with the so-called adjoint method for calculating the gradient of the cost function. We have examined the calculation of model inputs such as heat and freshwater fluxes, wind forcing, and mixing coefficients from hydrographic data. In addition, optimal estimates for the hydrography were obtained by requiring it to be consistent with both other types of data and the model dynamics. The velocity field calculated using the approach presented here is fully consistent with the model's dynamics; in particular, and unlike that often obtained by other inverse methods, it is mass conserving and satisfies all boundary conditions. These advantages are most useful as well as unique among presently used inverse techniques.

A main motivation for this study, other than demonstrating the technical feasibility of the method when applied to a full GCM, was to investigate possible difficulties that may be encountered when applying the method to real data and, in particular, to determine what data would be needed to determine the various model inputs. Such a study is most appropriately done using simulated data, where the "true" solution to the unknown model parameters is known and the performance of the method can be carefully examined under several different circumstances. We now briefly summarize our findings.

a. Deep convection

We have found that regions of deep convection pose a difficult problem, and the calculation of the model inputs, in particular the surface forcings, is extremely difficult in these regions. The optimization tends to fail in regions of deep convection when the model employs the commonly used convective-adjustment parameterization that mixes unstably stratified adjacent model levels. A more "gentle" parameterization, based on using a stratification-dependent vertical mixing coefficient that gradually increases when the stratification becomes unstable, results in improved performance of the optimization with noise-free ideal data, but does not eliminate the problem when noise is added to the simulated data. Two main reasons were suggested for these difficulties. First, the convective mixing of unstable stratification results in sharp changes to the cost function and its gradient and therefore prevents the optimization algorithm from converging to the right solution. In addition, the strong vertical mixing near the surface strongly amplifies the errors in the temperature and salinity fields, resulting in strong noise amplification for the calculated surface fluxes. Consequently, when analyzing real data using this method, flux estimates obtained using this methodology in regions of deep convection should be carefully interpreted.

b. Data needed to estimate surface fluxes and wind stress

Improving our knowledge of the surface forcings is certainly one of the important goals of oceanographic modeling due to their important role in the climate studies. Achieving this goal requires two main components: the appropriate available data that can be used to improve surface flux estimates, and a methodology that can link the available oceanographic data to the desired surface fluxes. The optimization approach together with the adjoint method for calculating the gradient of the cost function seems an appropriate tool linking the unknowns to be calculated and the various types of available data. But a remaining question of major importance is what data are needed to improve the surface flux estimates. To answer this question, we have made several optimizations using different types of simulated data and trying to calculate the wind stress and air–sea fluxes of heat and freshwater. Our results seem to indicate that hydrographic (temperature and salinity) data may be insufficient for obtaining optimal estimates of the surface wind stress. This may be expected to be a problem, especially where horizontal

advection is the dominant term in the tracer equations and the surface temperature and salinity fields do not contain independent information. The wind stress was efficiently and accurately calculated when surface ocean velocity data was made available to the optimization. Surface fluxes of heat and fresh water could be calculated from hydrographic data when no noise was present (i.e., with identical-twin data), but problems arose when noise was added to the simulated data.

Two possible reasons for the difficulties in calculating optimal estimates for the fluxes from noisy hydrographic data were mentioned: multiple local minima of the cost function and noise amplification due to ill conditioning of the inverse problem. We have used the rate of convergence of the optimization as a rough indicator of the conditioning of the inverse problem. We also explained that, beyond the preliminary exploration of this problem done here, simulated noisy data do not offer any real advantages over real oceanographic data for exploring the two aforementioned alternative explanations for the difficulties encountered. On the other hand, there is much to be learned by using real oceanographic data with the same methodology. In Part II of this work, North Atlantic data are therefore used to further analyze the difficulties found here with noisy simulated data, and in particular the problem of the conditioning of the inverse problem is discussed and analyzed in detail.

c. *Optimal hydrography*

Another goal of the present methodology, being a nonlinear inverse method, is to try to improve the possibly noisy hydrographic data while calculating the unknown model inputs. This seemed possible to do in the simulations done here, and turns out to be a crucial part of the optimization when applying the same methodology to the study of the North Atlantic Ocean in Part II.

The methodology used here is still rather new in the context of oceanographic data analysis, and there are many more issues that need further study and experimentation, both with real and simulated data. There are still many obstacles to overcome, but the method seems promising, and may be expected to become a useful tool of oceanographic data analysis. Developing the adjoint model required for inverting an oceanic GCM is a task that is far from being trivial, but once this is done (Long et al. 1989), it gives us a powerful method of assimilating observations and dynamics into a single consistent picture of the oceanic general circulation.

Acknowledgments. We wish to thank Kirk Bryan, Itzhak Feliks, and Irad Yavneh for most useful discussions at the stage of developing the GCM used here. This research was supported by Grant 89-00408 from the United States–Israel Binational Science Foundation.

APPENDIX

A Mixed Defect Correction Method for Solving the Singular Perturbation Equation for the Streamfunction

The equation (12) for the streamfunction that needs to be solved at every time step is a singular perturbation equation. Simple relaxation techniques like (SOR) cannot be used because the elliptic term in the equation is not dominant due to the small factor r multiplying it. The nonelliptic term resulting from the planetary and topographic β effects is dominant over most of the basin. To overcome this problem, we used an iterative method, that is, mixed defect correction iterations, suggested by Hemker (1984). Each iteration is composed of two stages, as follows.

Define an "artificial diffusion" operator similar to the operator acting on ψ in (12) except that r is replaced by a larger parameter α chosen so that the elliptic term in the equation is now dominant. Denote the resulting operator by L_α, while the original operator is denoted by L_r. During the first stage of the mth iteration, the following equation needs to be solved:

$$L_\alpha \psi^{m+1/2} = L_\alpha \psi^m - L_r \psi^m + Z(\lambda, \phi).$$

This is an elliptic equation for $\psi^{m+1/2}$ and is solved using SOR iterations. The second part of the mth iteration is a smoothing operation. Define D_α to be the diagonal part of L_α. That is, the operator D_α is simply the scalar factor multiplying ψ_{ij} in the finite-difference expression of $L_{\alpha\psi}$, evaluated at the horizontal location i, j. With this definition, the second half of the iteration involves solving the equation

$$D_\alpha \psi^{m+1} = D_\alpha \psi^{m+1/2} - L_\alpha \psi^{m+1/2} + Z(\lambda, \phi).$$

Now, the quantities ψ^m and $\psi^{m+1/2}$ converge to two different solutions. The desired solution for the streamfunction is the limit of ψ^m as $m \to \infty$. In practice, when starting a model run with a zero guess for ψ, several tens of iterations are needed to obtain a reasonable approximation. In following time steps, when the previous solution for ψ is used as a first guess, only a few (often just 1–2) mixed defect–correction iterations are needed.

REFERENCES

Bryan, K., 1969: A numerical method for the study of the circulation of the world ocean. *J. Comput. Phys.*, **4**, 347–376.

Bryan, K., and M. D. Cox, 1972: An approximate equation of state for numerical models of ocean circulation. *J. Phys. Oceanogr.*, **2**, 510–514.

Colin de Verdiere, A., 1988: Buoyancy driven planetary flows. *J. Mar. Res.*, **46**, 215–265.

Cox, M. D., 1984: A primitive equation 3 dimensional model of the ocean. GFDL Ocean Group Tech. Rep. No. 1, Princeton University, 137 pp.

Derber, J. C., 1985: The variational four dimensional assimilation of analyses using filtered models as constraints. Ph.D. dissertation, University of Wisconsin, Madison.

Gill, P. E., W. Murray, and M. H. Wright, 1981: *Practical Optimization.* Springer-Verlag, 377 pp.

Hemker, P. W., 1984: Mixed defect correction iteration for the solution of singular perturbation problems. *Computing,* **5**(Suppl), 123–145.

Le Dimet, F., and O. Talagrand, 1986: Variational algorithm for analysis and assimilation of meteorological observations: theoretical aspects. *Tellus,* **38A,** 97–110.

Long, R. B., and W. C. Thacker, 1989: Data assimilation into a numerical equatorial ocean model. I. The model and assimilation algorithm. *Dyn. Atmos. Oceans,* **13,** 379–412.

——, S.-M. Hwang, and W. C. Thacker, 1989: The finite-difference equations defining the GFDL-GCM and its adjoint. Unpublished report, Atlantic Oceanographic and Meteorological Laboratory, Miami, Florida.

Mercier, H., 1989: A study of the time averaged circulation in the western North Atlantic by simultaneous nonlinear inversion of hydrographic and current meter data. *Deep-Sea Res.,* **36,** 2, 297–313.

Numerical Algorithms Group, 1984: Fortran Library Manual, Mark II, 6 vols.

Olbers, D. J., M. Wenzel, and J. Willebrand, 1985: The inference of North Atlantic circulation patterns from climatological hydrographic data. *Rev. Geophys.,* **23,** 313–356.

Pacanowski, R., and S. G. H. Philander, 1981: Parameterization of vertical mixing in numerical models of tropical oceans. *J. Phys. Oceanogr.,* **11,** 1443–1451.

Provost, C., and R. Salmon, 1986: A variational method for inverting hydrographic data. *J. Mar. Res.,* **44,** 1–34.

Salmon, R., 1986: A simplified linear ocean circulation theory. *J. Mar. Res.,* **44,** 695–711.

Sarmiento, J. L., and K. Bryan, 1982: An ocean transport model for the North Atlantic. *J. Geophys. Res.,* **87,** 394–408.

Schröter, J., 1989: Driving of nonlinear time dependent ocean models by observation of transient tracers—a problem of constrained optimization. *Oceanic circulation models: combining data and dynamics,* Anderson and Willebrand, Eds., Kluwer Academic, 257–285.

Semtner, J. A., and M. R. Chervin, 1988: A simulation of the global ocean circulation with resolved eddies. *J. Geophys. Res.,* **93**(C), 15 502–15 522.

Sheinbaum, J., and D. L. T. Anderson, 1990: Variational assimilation of XBT data. Part I. *J. Phys. Oceanogr.,* **20,** 672–688.

Stommel, H., and F. Schott, 1977: The beta-spiral and absolute velocities in different oceans. *Deep-Sea Res.,* **24,** 325–329.

Thacker, W. C., 1989: The role of the Hessian matrix in fitting models to measurements. *J. Geophys. Res.,* **94,** 6177–6196.

——, and R. B. Long, 1988: Fitting dynamics to data. *J. Geophys. Res.,* **93,** C2, 1227–1240.

Tziperman, E., and W. C. Thacker, 1989: An Optimal Control/Adjoint equations approach to studying the oceanic general circulation. *J. Phys. Oceanogr.,* **19,** 1471–1485.

——, ——, and K. Bryan, 1992: Computing the steady state oceanic circulation using an optimization approach. *Dyn. Atmos. Oceans,* **16,** 379–403.

——, ——, R. B. Long, Show-Ming Hwang, and S. Rintoul, 1992: Oceanic data analysis using a general circulation model. Part II: A North Atlantic model. *J. Phys. Oceanogr.,* **22,** 1458–1485.

Wunsch, C., 1978: The general circulation of the North Atlantic west of 50°W determined from inverse methods. *Rev. Geophys.,* **16,** 583–620.

——, 1988: Transient tracers as a problem in control theory. *J. Geophys. Res.,* **93,** C7, 8099–8110.